NATIONAL ADVISORY COMMITTEE FOR AERONAUTICS

TECHNICAL MEMORANDUM 1343

THE EXCITATION OF UNSTABLE PERTURBATIONS IN A LAMINAR FRICTION LAYER

By J. Pretsch

Translation of "Die Anfachung instabiler Störungen in einer laminaren Reibungsschicht." Bericht der Aerodynamischen Versuchsanstalt Göttingen E. V., Institut für Forschungsflugbetrieb und Flugwesen, Jahrbuch der deutschen Luftfahrtforschung, August 1942.

NACA
Washington
September 1952

1A

NATIONAL ADVISORY COMMITTEE FOR AERONAUTICS

TECHNICAL MEMORANDUM 1343

THE EXCITATION OF UNSTABLE PERTURBATIONS IN A LAMINAR FRICTION LAYER*

By J. Pretsch

With the aid of the method of small oscillations which was used successfully in the investigation of the stability of laminar velocity distributions in the presence of two-dimensional perturbations, the excitation of the unstable perturbations for the Hartree velocity distributions occurring in plane boundary-layer flow for decreasing and increasing pressure is calculated as a supplement to a former report. The results of this investigation are to make a contribution toward calculation of the transition point on cylindrical bodies.

OUTLINE

---

*"Die Anfachung instabiler Störungen in einer laminaren Reibungsschicht." Bericht der Aerodynamischen Versuchsanstalt Göttingen E. V., Institut für Forschungsflugbetrieb und Flugwesen, Jahrbuch der deutschen Luftfahrtforschung, August 1942, p. I54-I71.

I. STATEMENT OF THE PROBLEM

If one wants to make a theoretical calculation of the profile drag of bodies in a flow for a certain direction of air flow, one must know - in addition to the pressure distribution - the position of the transition zone where the laminar boundary layer becomes turbulent. The separation point of the laminar layer forms a rearward limit for the transition point on a section of this body surrounded by the flow. It lies in the region of the pressure increase at the point where the velocity distribution in the boundary layer has the wall shearing stress zero. This separation point is a fixed point of the profile in the flow, the position of which does not shift due to a variation of the Reynolds number $Re = \frac{U_\infty t}{\nu}$ (U_∞ = velocity of air flow, t = chord of the body). One may calculate it according to the well-known approximation method of Pohlhausen which, for prescribed pressure distribution, provides for every profile point a velocity distribution of the boundary layer with a certain form parameter λ ($\lambda = -12$ separation). As forward limit for the transition point, one may take the stability limit of the laminar layer with respect to small two-dimensional perturbations which were calculated in references 2 and 3 according to the method developed by W. Tollmien (ref. 1). According to this method, there exists for every form of velocity distribution in the boundary layer a so-called critical Reynolds number $Re^*_{cr} = \left(\frac{U_a \delta^*}{\nu}\right)_{cr}$ (U_a = local potential velocity, δ^* = local displacement thickness) below which all perturbations are damped; its value increases as the form of the velocity profile becomes fuller (with increasing λ). Where the Reynolds number $Re^* = \frac{U_a \delta^*}{\nu}$ formed with the actual potential velocity U_a and the actual displacement thickness δ^* exceeds this critical Reynolds number, there begins the instability of the boundary layer. In contrast to the laminar separation point, this stability limit is therefore not fixed on the profile for a normal pressure distribution but travels forward toward the stagnation point on bodies in flows with increasing Reynolds number Re (see fig. 1).

The actual transition point which lies between these two limits - stability limit and separation point - is known to likewise shift forward with increasing Reynolds number Re. That it lies only a certain distance behind the stability limit (as shown by a comparison of experimental transition points and theoretical stability limits) is plausible, because the excitation of the unstable perturbations starts only at this limit point of the stability and must obviously have attained a certain degree before the instability further downstream leads to the breakdown of the laminar flow configuration.

For this reason it seemed necessary to calculate, or at least to estimate, for the velocity distributions in the laminar boundary layer in the entire instability range of the latter, the excitation of the unstable perturbations as well, with the objective of making an improved calculation of the transition point possible.

For the velocity distribution on the flat plate in longitudinal flow (Blasius profile), H. Schlichting (ref. 4) has already determined the excitation quantity as a function of perturbation frequency and Reynolds number in a part of the instability range; and for the velocity distributions in the region of pressure increase, W. Tollmien (ref. 5) has explained the behavior of the excitation (in first asymptotic approximation for very large Reynolds numbers) in a very general manner, neglecting the effects of internal friction.

II. THE GENERAL DIFFERENTIAL EQUATION DESCRIBING THE PERTURBATION

Since the bases for the method of stability investigation have been discussed in detail in an earlier report (ref. 3), we can refer to the results attained there.

Let $U(x,y)$ and $V(x,y)$ be the tangential and normal components of a plane steady boundary-layer flow; let x denote the length of the arc and y the normal to the profile contour. The stream function of the two-dimensional perturbation motion which we superpose on this basic flow is assumed to be

$$\left.\begin{aligned} \Psi(x,y,t) &= \varphi(x,y)e^{i\alpha(x-ct)} = \varphi(x,y)e^{\beta_i t}e^{i(\alpha x-\beta_r t)} \\ c &= c_r + ic_i \qquad \beta_i = c_i\alpha \qquad \beta_r = c_r\alpha \end{aligned}\right\} \tag{1}$$

here t denotes the time, α the spatial circular frequency of the perturbation, the real part c_r of c its phase velocity, and the imaginary part c_i a measure for its excitation ($c_i > 0$) or damping ($c_i < 0$); besides β_i is the logarithmic increment of the excitation of the perturbation amplitude, and β_r the circular frequency in time of the perturbation.

If we substitute the motion originating by superposition of the boundary-layer flow U, V, and the perturbation motion

$$\left.\begin{aligned} \bar{u} &= \frac{\partial \psi}{\partial y} = \varphi' e^{i\alpha(x-ct)} \\ \bar{v} &= -\frac{\partial \psi}{\partial x} = -\left(i\alpha\varphi + \frac{\partial \varphi}{\partial x}\right) e^{i\alpha(x-ct)} \end{aligned}\right\} \tag{2}$$

into Navier-Stokes' differential equations, we obtain - as was proved in reference 3 in detail - the differential equation describing the perturbation in the form

$$\left.\begin{aligned} (U-c)\left(\varphi'' - \alpha^2\varphi\right) - U''\varphi &= \frac{-i}{\alpha \mathrm{Re}^*}\left(\varphi^{IV} - 2\alpha^2\varphi'' + \alpha^4\varphi\right) \\ \mathrm{Re}^* &= \frac{U_a \delta^*}{\nu} \end{aligned}\right\} \tag{3}$$

Here the prime (') denotes differentiation with respect to the wall distance y; the velocities are referred to the local velocity U_a at the boundary-layer limit, and the wall distance as well as the wave length $\Lambda = \frac{2\pi}{\alpha}$ are referred to the local displacement thickness δ^*.

In order to avoid misunderstandings it should again be emphasized that - in spite of the assumption that U, V, and φ be functions of the arc length x - only the form of the local velocity distribution is decisive for the stability investigation as one recognizes from equation (3). The immediate effect of the pressure gradient, however, is negligibly small as is also the influence of the x-dependence of the perturbation amplitude φ.

The boundary conditions of the differential equation (3) result from the condition that the perturbation velocities $\bar{u}$, $\bar{v}$ vanish at the wall and that the friction effect at the outer boundary-layer limit ($U'' = 0$) has disappeared. With their aid, the calculation of the excitation of the unstable perturbations may be reduced to an eigenvalue problem, the solution of which is discussed in section V.

We deal first with establishing the particular solutions of the differential equation (3), limiting ourselves to small values of the

excitation quantity c_i; thus, the general solution of the differential equation describing the perturbation (3) may be represented in the form

$$\varphi^* = \sum_{\nu=1}^{4} C_\nu^* \varphi_\nu^* = \sum_{\nu=1}^{4} C_\nu^* \left(\varphi_\nu - \frac{ic_i}{U_0'} \omega_\nu \right) \qquad U_0' = U'_{U=c} \tag{4}$$

There φ_ν denotes the particular solutions for $c_i = 0$ which are obtained in the calculation of the limiting curve of the instability range (neutral curve) in the α, Re^*-plane (ref. 3), and the ω_ν signifies additional functions for $c_i > 0$.

We turn first to calculating the integrals φ_1^*, φ_2^* and the additional functions ω_1, ω_2.

III. THE SOLUTIONS φ_1^*, φ_2^* OF THE DIFFERENTIAL EQUATION DESCRIBING THE FRICTIONLESS PERTURBATION FOR FINITE EXCITATION

If αRe^* is assumed to be very large, the differential equation (3) is simplified to the so-called frictionless-perturbation equation

$$(U - c)(\varphi'' - \alpha^2 \varphi) - U''\varphi = 0 \tag{5}$$

This differential equation has a pole of the first order at the location $U = c = c_r + ic_i$ to which we coordinate the point y_c^* of the complex y-plane. In the neighborhood of this singularity, a fundamental system may be easily indicated by series development. In order to establish the connection with the case of the purely real c treated before (see ref. 3), we first give the relation between the complex y_c^* and the wall distance y_c of the "critical" layer $U = c_r$.

From

$$U(y_c) = c_r \tag{6}$$

and

$$U\left(y_c^*\right) = c_r + ic_i \tag{7}$$

there follows

$$U\left(y_c^*\right) - U(y_c) = ic_i = \left(y_c^* - y_c\right)U_0' + \ldots \tag{8}$$

and, with limitation to the terms linear in c_i, therefore

$$y^* = y_c + \frac{ic_i}{U_0'} \tag{9}$$

We shall now indicate the construction of the solutions φ_1^*, φ_2^* of equation (5) for those special velocity distributions U(y) by which we shall approximate the laminar boundary profiles of Hartree (ref. 6) for the calculation of the excitation of the unstable perturbations in the same manner as we did before in reference 3 for the calculation of their critical Reynolds numbers.

(a) Binomial Velocity Distribution (Pressure Decrease)

In the region of the pressure decrease, we used the approximation function

$$U = 1 - (a - y)^n \qquad n = 2,3,4, \ldots \tag{10}$$

where a denotes the coordinate of the point of junction to the potential velocity.

With the new variable

$$y_1 = \frac{y - y_c}{a - y_c} \tag{11}$$

and with

$$\alpha_1 = \alpha(a - y_c) \tag{12}$$

the perturbation equation (5) for indifferent perturbations then reads

$$\left[1 - (1 - y_1)^n\right]\left(\frac{d^2\varphi}{dy_1^2} - \alpha_1^2\varphi\right) + n(n - 1)(1 - y_1)^{n-2}\varphi = 0 \tag{13}$$

Using the relations (9) and (11), we now introduce the complex variable

$$y_1^* = \frac{y - y_c^*}{a - y_c} = y_1 + \frac{y_c - y_c^*}{a - y_c} = y_1 - \frac{ic_i}{U_0'(a - y_c)} \tag{14}$$

With the abbreviation

$$f_1 = -\frac{c_i}{U_0'(a - y_c)} = \frac{c_i}{n(c_r - 1)} \tag{15}$$

the differential equation describing the frictionless perturbation for nondisappearing excitation then is transformed into the form

$$\left[1 - \left(1 - y_1^*\right)^n + nif_1\left\{1 - (1 - y)^{n-1}\right\}\right]\left(\frac{d^2\varphi^*}{dy_1^2} - \alpha_1^2\varphi^*\right) +$$

$$n(n - 1)\left[\left(1 - y_1^*\right)^{n-2} + (n - 2)if_1\left(1 - y_1^*\right)^{n-3}\right]\varphi^* = 0 \tag{16}$$

in which, according to our presupposition, only the terms linear in f_1 have been taken into consideration.

If one writes equation (16) after multiplication by

$$\frac{y_1^{*2}}{1 - \left(1 - y_1^*\right)^n + nif_1\left[1 - \left(1 - y_1^*\right)^{n-1}\right]}$$

and after division in the form

$$y_1^{*2} \frac{d^2\varphi^*}{dy_1^{*2}} + \varphi^* \sum_{i=1}^{\infty} \beta_i^* y_1^{*i} = 0 \tag{17}$$

the first solution φ_1^* is given by

$$\frac{\varphi_1^*}{a - y_c} = y_1^* \sum_{\nu=0}^{\infty} e_\nu^* y_1^{*\nu} = \frac{1}{a - y_c}\left(\varphi_1 - \frac{ic_i}{U_0'} \omega_1\right) \tag{18}$$

with

$$\omega_1 = \sum_{\nu=0}^{\infty} g_\nu y_1^\nu \tag{19}$$

The series coefficients e_ν^* are obtained from the β_ν^* according to the recursion formula

$$\nu(\nu + 1)e_\nu^* + \sum_{\mu=0}^{\nu=1} \beta_{\nu-\mu}^* e_\mu^* = 0 \qquad e_0^* = 1 \tag{20}$$

The solution φ_2^* for all y_1^* is found to be

$$q_2^* = \varphi_1^* \int \frac{1}{\varphi_1^{*2}}\, dy = 1 + \sum_{\nu=2}^{\infty} b_\nu^* y_1^{*\nu} + 2e_1^* \frac{\varphi_1^*}{a - y_c} \ln y_1^* \tag{21}$$

In this equation, the logarithms are, however, ambiguous; one must cut the complex y_1^*-plane in such a manner that

$$-\frac{3}{2}\pi < \arg y_1^* < \frac{\pi}{2}$$

If we put

$$\sum_{\nu=2}^{\infty} b_\nu^* y_1^{*\nu} = \sum_{\nu=2}^{\infty} b_\nu y_1^\nu + if_1 \sum_{\nu=1}^{\infty} h_\nu y_1^\nu \tag{22}$$

φ_2^* may be represented for y_1 = real part of $y_1^* > 0$ at first in the form

$$\varphi_2^* = 1 + \sum_{\nu=2}^{\infty} b_\nu y_1^\nu + if_1 \sum_{\nu=1}^{\infty} h_\nu y_1^\nu +$$

$$2e_1\left(1 - if_1\right)\left(\frac{\varphi_1}{a - y_c} + if_1 \sum_{\nu=0}^{\infty} g_\nu y_1^\nu\right)$$

$$\left(\ln y_1 + \frac{if_1}{y_1}\right) = \varphi_2 - \frac{ic_i}{U_0'}\omega_2 \tag{23}$$

with

$$\omega_2 = \frac{1}{a - y_c}\left[\sum_{\nu=1}^{\infty} h^\nu y_1^\nu + \frac{2e_1\varphi_1}{a - y_c}\left(\frac{1}{y_1} - \ln y_1\right) + \right.$$

$$\left. 2e_1 \ln y_1 \sum_{\nu=0}^{\infty} g_\nu y_1^\nu\right] \tag{24}$$

In the transformation of equation (21) into equation (23) the relation

$$e_1^* = e_1(1 - if_1) \tag{25}$$

is put to use; it is easily obtained from the perturbation equation (5) if $U(y)$ and φ_1^* for $c_i = 0$, and for $c_i = 0$ in the neighborhood of the singularity $U = c$ are developed into a Taylor series, since

$$2e_1 = (a - y_c)\frac{U_0''}{U_0'} \tag{26}$$

and

$$2e_1^* = (a - y_c)\frac{U_0'' + ic_i\frac{U_0'''}{U_0'}}{U_0' + ic_i\frac{U_0''}{U_0'}}$$

$$\sim (a - y_c)\frac{U_0''}{U_0'}\left[1 - \frac{ic_i}{U_0'}\left(\frac{U_0''}{U_0'} - \frac{U_0'''}{U_0''}\right)\right]$$

$$= (a - y_c)\frac{U_0''}{U_0'}(1 - if_1) \tag{27}$$

If we express in equation (27) the exact value

$$\left(\frac{U_0''}{U_0'} - \frac{U_0'''}{U_0''}\right)$$

again by the approximate value f_1, this step is motivated by the fact that due to the small value of c_i, one deals here only with a correction term for the value of $\frac{U_0''}{U_0'}$.

For $y_1 < 0$, φ_2^* is represented by the expression

$$\varphi_2^* = 1 + \sum_{\nu=2}^{\infty} b_\nu^* y_1^{*\nu} + 2e_1^* \frac{\varphi_1^*}{a - y_c}\left(\ln\left|y_1^*\right| + i \arg y_1^*\right)$$

$$= \varphi_2 - \frac{ic_i}{U_0'}\omega_2 \qquad \left(-\frac{3}{2}\pi < \arg y^* < \frac{\pi}{2}\right) \tag{28}$$

with

$$\omega_2 = \frac{1}{a - y_c}\left\{\left[\sum_{\nu=1}^{\infty} h_\nu y_1^\nu + \frac{2e_1\varphi_1}{a - y_c}\left(\frac{1}{y_1} - \ln\left|y_1\right|\right) + 2e_1 \ln\left|y_1\right| \sum_{\nu=0}^{\infty} g_\nu y_1^\nu\right] + 2i\pi e_1\left(\frac{\varphi_1}{a - y_c} - \sum_{\nu=0}^{\infty} g_\nu y_1^\nu\right)\right\} \tag{29}$$

The term with $i \arg y_1^*$ in equation (28) was obtained by H. Schlichting (ref. 4) and W. Tollmien (ref. 5) by a discussion of the general perturbation equation (3) in the neighborhood of the singularity $U = c_r + ic_i$ in a similar manner as the "transition substitution" in the critical layer for purely real c by taking the friction effect into consideration.

Since we are, in the calculation of the transition substitution, concerned with a representation of e_1 of maximum accuracy, we shall replace e_1 by the expression (26) of the Taylor development of the exact Hartree profile.

For the linear and the parabolic approximate distribution [$n = 1$, $n = 2$ in equations (10) and (16)] H. Schlichting (ref. 4) has already given the solutions φ_1^*, φ_2^*. This calculation was continued for $n = 3$ and $n = 4$. The coefficients β_ν^*, e_ν^*, b_ν^*, g_ν, h_ν are compiled numerically in table 1. For the convergence of the power series, the reflections made in reference 3 are valid.

(b) Sinusoidal Velocity Distribution (Pressure Increase)

In the region of pressure increase, the Hartree velocity distributions in the boundary layer (see ref. 3) were approximated by formulation in terms of a sine formula introduced by W. Tollmien (ref. 5).

$$U = U_s + (1 - U_s)\sin\left(\frac{y - s}{a - s}\frac{\pi}{2}\right) \tag{30}$$

where s denotes the wall distance of the inflection point.

With the new real variable

$$y_2 = \frac{\pi}{2}\frac{y - y_c}{a - s} \tag{31}$$

and with

$$\alpha_2 = \frac{2}{\pi}(a - s)\alpha \tag{32}$$

the perturbation equation (5) for the indifferent perturbations then read

$$\left[\sin\left(y_2 - y_{2s}\right) + \sin y_{2s}\right]\left(\frac{d^2\varphi}{dy_2^2} - \alpha_2^2\varphi\right) + \sin\left(y_2 - y_{2s}\right)\varphi = 0 \tag{33}$$

where y_{2s} was put equal to

$$y_{2s} = \frac{\pi}{2} \frac{s - y_c}{a - s} \tag{34}$$

We now introduce the complex variable

$$y_2^* = \frac{\pi}{2} \frac{y - y_c^*}{a-s} = y_2 + \frac{\pi}{2} \frac{y_c - y_c^*}{a - s} = y_2 - \frac{ic_i}{U_0'} \frac{\pi}{2(a - s)} \tag{35}$$

With the abbreviation

$$f_2 = - \frac{c_i}{U_0'} \frac{\pi}{2(a - s)} = - \frac{c_i}{(1 - U_s)\cos y_{2s}} \tag{36}$$

the frictionless differential equation, describing the perturbation for non-vanishing excitation, then is transformed into

$$\left[\sin\left(y_2^* - y_{2s}\right) + \sin y_{2s} - if_2\left\{\cos\left(y_2^* - y_{2s}\right) - \cos y_{2s}\right\}\right]$$
$$\left(\frac{d^2\varphi^*}{dy_2^{*2}} - \alpha_2^2\varphi^*\right) + \left[\sin\left(y_2^* - y_{2s}\right) - if_2 \cos\left(y_2^* - y_{2s}\right)\right]\varphi^* = 0 \tag{37}$$

If (37) is written like equation (16) in the form

$$y_2^{*2} \frac{d^2\varphi^*}{dy_2^{*2}} + \varphi^* \sum_{i=1}^{\infty} \beta_i^* y_2^{*i} = 0 \tag{38}$$

the solutions φ_1^*, φ_2^* are determined by analogy with the equations (18), (23), and (28). One has

$$\frac{\pi}{2(a - s)} \varphi_1^* = y_2^* \sum_{\nu=0}^{\infty} e_\nu^* y_2^{*\nu} = \frac{\pi}{2(a - s)}\left(\varphi_1 - \frac{ic_i}{U_0'} \omega_1\right) \tag{39}$$

with

$$\omega_1 = \sum_{\nu=0}^{\infty} g_\nu y_2^\nu \tag{40}$$

For $y_2 > 0$, the solution φ_2 is obtained

$$\varphi_2^* = 1 + \sum_{\nu=2}^{\infty} b_\nu^* y_2^{*\nu} + 2e_1^* \frac{\pi\varphi_1^*}{2(a - s)} \ln y_2^*$$

$$\left(-\frac{3}{2}\pi < \arg y_2^* < \frac{\pi}{2}\right) \tag{41}$$

If one puts

$$\sum_{\nu=2}^{\infty} b_\nu^* y_2^{*\nu} = \sum_{\nu=2}^{\infty} b_\nu y_2^\nu + if_2 \sum_{\nu=1}^{\infty} h_\nu y_2^\nu \tag{42}$$

φ_2^* for $y_2 > 0$ may be represented in the form

$$\varphi_2^* = 1 + \sum_{\nu=2}^{\infty} b_\nu y_2^\nu + if_2 \sum_{\nu=1}^{\infty} h_\nu y_2^\nu + 2e_1\left(1 + \frac{if_2}{\sin y_{2s} \cos y_{2s}}\right)$$

$$\left(\frac{\pi\varphi_1}{2(a - s)} + if_2 \sum_{\nu=0}^{\infty} g_\nu y_2^\nu\right)\left(\ln y_2 + \frac{if_2}{y_2}\right)$$

$$= \varphi_2 - \frac{ic_i}{U_0'} \omega_2 \tag{43}$$

with

$$\omega_2 = \frac{\pi}{2(a - s)}\left[\sum_{\nu=1}^{\infty} h_\nu y_2^\nu + \frac{2\pi e_1 \varphi_1}{2(a - s)}\left(\frac{1}{y_2} + \frac{\ln y_2}{\sin y_{2s} \cos y_{2s}}\right) + 2e_1 \ln y_2 \sum_{\nu=0}^{\infty} g_\nu y_2^\nu\right] \tag{44}$$

In transforming (41) into (43), one makes use of the relation

$$e_1^* = e_1\left(1 + \frac{if_2}{\sin y_{2s} \cos y_{2s}}\right) \tag{45}$$

which follows from the two equations

$$e_1 = \frac{a - s}{\pi} \frac{U_0''}{U_0'} \tag{46}$$

and

$$\begin{aligned} e_1^* &= \frac{(a - s)}{\pi} \frac{U_0'' + ic_i \frac{U_0'''}{U_0'}}{U_0' + ic_i \frac{U_0''}{U_0'}} \\ &\sim \frac{(a - s)}{\pi} \frac{U_0''}{U_0'} \left[1 - \frac{ic_i}{U_0'}\left(\frac{U_0''}{U_0'} - \frac{U_0'''}{U_0''}\right)\right] \\ &= \frac{(a - s)}{\pi} \frac{U_0''}{U_0'}\left(1 + \frac{if_2}{\sin y_{2s} \cos y_{2s}}\right) \end{aligned} \tag{47}$$

φ_2^* for $y_2 < 0$, is represented by the expression

$$\begin{aligned} \varphi_2^* &= 1 + \sum_{\nu=2}^{\infty} b_\nu^* y_2^{*\nu} + e_1^* \frac{\pi}{(a - s)} \varphi_1^*\left(\ln\left|y_2^*\right| + i \arg y_2^*\right) \\ &= \varphi_2 - \frac{ic_i}{U_0'} \omega_2 \qquad \left(-\frac{3}{2}\pi < \arg y_2^* < \frac{\pi}{2}\right) \end{aligned} \tag{48}$$

with

$$\omega_2 = \frac{\pi}{2(a - s)}\left\{\left[\sum_{\nu=1}^{\infty} h_\nu y_2^\nu + \frac{\pi e_1 \varphi_1}{a - s}\left(\frac{1}{y_2} + \frac{\ln y_2}{\sin y_{2s} \cos y_{2s}}\right) + 2e_1 \ln\left|y_2\right| \sum_{\nu=0}^{\infty} g_\nu y_2^\nu\right] + 2i\pi e_1\left(\frac{-\pi\varphi_1}{2(a - s) \sin y_{2s} \cos y_{2s}} - \sum_{\nu=0}^{\infty} g_\nu y_2^\nu\right)\right\} \tag{49}$$

For the calculation of the transition substitution, we shall replace the term e_1, as in section III(a), by the accurate value (equation (46)) of the Taylor development of the exact Hartree profile.

In a comparison of the relations (24) and (44) or (27) and (47) or (29) and (49), it is striking that, in the expressions for e_1^* and ω_2 for the sinusoidal boundary-layer profiles in case of pressure increase, the product $\sin y_{2s} \cos y_{2s}$ appears in the denominator of several terms. The sign of this product is negative when the inflection point of the velocity distribution lies more closely to the wall than the critical layer $\left(y_{2s} < 0\right)$; the critical layer thus lies in the part of the velocity profile showing concave curvature. The sign of the expressions divided by $\sin y_{2s} \cos y_{2s}$ then is the same as the sign of the corresponding terms in the solutions for the velocity distributions in case of pressure decrease which, as is known, have concave curvature at every wall distance. If, in contrast, the critical layer is located between point of inflection and wall $\left(y_{2s} > 0\right)$, then, in the part of the velocity profile having convex curvature the signs discussed are reversed. In that case, when the critical layer shifts to the point of inflection itself $\left(y_{2s} = 0\right)$, the behavior of e_1^* and ω_2 is regular since then

$$e_1^* = -\frac{ic_i}{2(1 - U_s)} = \frac{if_2}{2} \tag{50}$$

and

$$\omega_{2(y_c = s)} = \frac{\pi}{2(a - s)}\left[\sum_{\nu=1}^{\infty} h_\nu y_2{}^\nu + \frac{\pi\varphi_1}{2(a - s)} \ln y_2\right] \qquad (y_2 > 0) \tag{51}$$

$$\omega_{2(y_c = s)} = \frac{\pi}{2(a - s)}\left\{\left[\sum_{\nu=1}^{\infty} h_\nu y_2{}^\nu + \frac{\pi\varphi_1}{2(a - s)} \ln|y_2|\right] - \frac{i\pi^2\varphi_1}{2(a - s)}\right\} \qquad (y_2 < 0) \tag{52}$$

The series coefficients $\beta_\nu{}^*$, $e_\nu{}^*$, $b_\nu{}^*$, g_ν, h_ν for the sinusoidal basic velocity are given numerically in table 2. For the convergence of the series developments, the explanations of the earlier report (ref. 3) are again valid.

IV. THE FRICTION SOLUTION $\varphi_3{}^*$ FOR FINITE EXCITATION

Besides playing a role in the critical layer $U = c$, the friction of the fluid is of importance also in the neighborhood of the wall where it occasions two more solutions $\varphi_3{}^*$, $\varphi_4{}^*$ of the general differential equation describing the perturbation (3).

If we introduce the variable

$$\eta^* = \frac{y - y_c{}^*}{\epsilon^*} \tag{53}$$

with

$$\epsilon^* = \left[\alpha Re^*\left(U_0' + ic_i \frac{U_0''}{U_0'}\right)\right]^{-1/3} \tag{54}$$

we obtain from equation (3) in the limiting process $\epsilon \longrightarrow 0$ for large Reynolds numbers the differential equation

$$\frac{id^4\varphi_{3,4}^*}{d\eta^{*4}} + \eta^* \frac{d^2\varphi_{3,4}^*}{d\eta^{*2}} = 0 \tag{55}$$

The solutions of this differential equation are just as independent of the form of the velocity distribution $U(y)$ as was the case for the solutions φ_3, φ_4 for the excitation zero (ref. 1); they read corresponding to reference 2:

$$\varphi_{3,4}^* = \int_{\infty}^{\eta^*} d\eta^* \int_{\infty}^{\eta^*} \eta^{*1/2} H_{1/3}^{(1),(2)} \left[\frac{2}{3}\left(i\eta^*\right)^{3/2}\right] d\eta^* \tag{56}$$

where $H^{(1),(2)}$ signifies the Hankel function of the first and second kind, respectively.

Since the Hankel function of the first kind increases for large wall distance beyond all limits, it cannot be contained in the general integral (4) so that we there may put $C_4 = 0$.

V. STATEMENT AND SOLUTION OF THE EIGENVALUE PROBLEM

After having found the particular solutions of the differential equation describing the perturbation (3), we now state the eigenvalue problem, (which results from the boundary conditions of the perturbation equation) for investigation of the excitation of the unstable perturbations.

At the wall, the tangential as well as the normal component of the perturbation velocity disappear; thus one has

$$C_1^*\varphi_1^*{}_w + C_2^*\varphi_2^*{}_w + C_3^*\varphi_3^*{}_w = 0 \tag{57}$$

$$C_1^*\varphi_1^*{}_w' + C_2^*\varphi_2^*{}_w' + C_3^*\varphi_3^*{}_w' = 0 \tag{58}$$

At the point of juction $y = a$ to the region of constant velocity, U'' is zero and therewith $\varphi^{*''} - \alpha^2\varphi^* = 0$, that is $\varphi^* = e^{-\alpha y}$, so that the third boundary condition reads

$$C_1^*\Phi_1^*{}_a + C_2^*\Phi_2^*{}_a = 0 \tag{59}$$

with

$$\Phi_\nu^*{}_a = \varphi_\nu^*{}_a' + \alpha\varphi_\nu^*{}_a, \quad \nu = 1, 2, \ldots \tag{60}$$

A term Φ_{3a}^* does not appear because the particular friction solution φ_3^* has already been damped at the point of junction.

In order that the three homogeneous equations (57), (58), and (59) may have a solution different from zero, the determinant must disappear

$$\begin{vmatrix} \varphi_1^*{}_w & \varphi_2^*{}_w & \varphi_3^*{}_w \\ \varphi_1^*{}_w' & \varphi_2^*{}_w' & \varphi_3^*{}_w' \\ \Phi_1^*{}_a & \Phi_2^*{}_a & 0 \end{vmatrix} = 0 \tag{61}$$

The solution of this determinant yields the equation

$$\frac{\varphi_3^*{}_w}{\varphi_3^*{}_w'} = \frac{\varphi_2^*{}_w\Phi_1^*{}_a - \varphi_1^*{}_w\Phi_2^*{}_a}{\varphi_2^*{}_w'\Phi_1^*{}_a - \varphi_1^*{}_w'\Phi_2^*{}_a} \tag{62}$$

or with Schlichting's abbreviations

$$\frac{1}{\epsilon^*\eta_0^*}\frac{\varphi_3^*{}_w}{\varphi_3^*{}_w'} = -\frac{D(\eta_0^*)}{\eta_0^*} = F(\eta_0^*) = F^* \tag{63}$$

$$-\frac{1}{y_c^*}\frac{\varphi_2^* w \Phi_1^* a - \varphi_1^* w \Phi_2^* a}{\varphi^*{}_w' \Phi_1^* a - \varphi_1^* w' \Phi_2^* a} = E^*(\alpha, c_r, c_i) \tag{64}$$

finally

$$F^* = E^*(\alpha, c_r, c_i) \tag{65}$$

Therein

$$\eta_0^* = -\frac{y_c^*}{\epsilon^*} \tag{66}$$

The complex equation (65) is equivalent to two real equations in which the parameters α, Re^*, c_r, and c_i are contained. If one limits oneself to the case of indifferent perturbations ($c_i = 0$), one obtains from them after elimination of c_r a relation between the Reynolds number Re^* and the wave length $\frac{2\pi}{\alpha}$ of the perturbation. That is the equation of the neutral curve or the curve of constant zero excitation by which the stable and unstable perturbation states are separated and the lowest Reynolds number of which is the so-called critical Reynolds number Re^*_{cr}; when this critical Reynolds number is exceeded, the excitation of the unstable perturbations begins.

These neutral curves were determined in a previous report (ref. 3) for the velocity profiles for decreasing and for increasing pressure calculated by Hartree.

In the present investigation, we shall assume the excitation quantity c_i to be different from zero and investigate the curves of constant excitation enclosed by this neutral curve.

For this purpose, we shall solve the complex equation (65) in a somewhat simpler manner than Schlichting (ref. 4), by determining not the differential quotients $\frac{\partial c_i}{\partial \alpha}$ and $\frac{\partial c_i}{\partial Re^*}$ at the location of the neutral curve, but the curves of constant excitation $c_i > 0$ directly by a method similar to that applied for the neutral curve $c_i = 0$; however, without making use of this curve itself. We consider first the left side of equation (65).

Since we intend to limit ourselves to small values of excitation, we develop F^* in the form

$$F^* = F\left(\eta_0{}^*\right) = F\left(\eta_0\right) + \left(\eta_0{}^* - \eta_0\right)\left(\frac{dF}{d\eta_0{}^*}\right)_{\eta_0{}^*=\eta_0} + \ldots \tag{67}$$

where η_0 as before in reference 1 is defined by the relation

$$\eta_0 = - y_c\left(\alpha Re^* U_0{}'\right)^{+1/3} \tag{68}$$

According to equations (9), (54), (66), and (68) one now has

$$\begin{aligned}\eta_0{}^* &= - y_c\left(1 + \frac{ic_i}{U_0{}'y_c}\right)\left[\alpha Re^* U_0{}'\left(1 + \frac{ic_i U_0{}''}{U_0{}'^2}\right)\right]^{1/3} \\ &\sim - y_c\left(\alpha Re^* U_0{}'\right)^{1/3}\left[1 + \frac{ic_i}{U_0{}'y_c}\left(1 + \frac{y_c}{3}\frac{U_0{}''}{U_0{}'}\right)\right] \\ &= \eta_0\left[1 + \frac{ic_i}{U_0{}'y_c}\left(1 + \frac{y_c}{3}\frac{U_0{}''}{U_0{}'}\right)\right]\end{aligned} \tag{69}$$

Thus equation (67) becomes

$$\begin{aligned}F^* = F\left(\eta_0{}^*\right) &\sim F\left(\eta_0\right) + \frac{ic_i}{U_0{}'y_c}\eta_0\left(1 + \frac{y_c}{3}\frac{U_0{}''}{U_0{}'}\right)\frac{dF}{d\eta_0} \\ &= G\left(\eta_0, c_r, c_i\right)\end{aligned} \tag{70}$$

One sees therefore that the form of velocity distribution which does not enter into the exact solution $F(\eta_0^*)$ according to equations (63) and (56) does appear explicitly in the development of $F(\eta_0^*)$ with respect to c_i.

The differential quotient

$$\frac{dF}{d\eta_0} = \frac{dF_r}{d\eta_0} + i\frac{dF_i}{d\eta_0}$$

was determined by graphic differentiation of the function $F(\eta_0)$. The numerical values of its real and imaginary part are given numerically in table 3. Since real and imaginary parts nowhere disappear simultaneously, the function $F(\eta_0^*)$ will be free from singularities in region around the function $F(\eta_0)$ and the development (67) will be thus permissible.

We now consider the right side of equation (65) which is defined by the relation (64).

Remembering the splitting of the frictionless solutions $\varphi_\nu^*(\nu = 1,2)$ in the form of equation (4), we first put

$$\Phi_\nu^*{}_a = \Phi_{\nu a} - \frac{ic_i}{U_0'}\Omega_{\nu a}$$

with

$$\left.\begin{aligned} \Omega_{\nu a} &= \omega_{\nu a}' + \alpha\omega_{\nu a} \\ \text{furthermore} \qquad \varphi_\nu^*{}_w &= \varphi_{\nu w} - \frac{ic_i}{U_0'}\omega_{\nu w} \end{aligned}\right\} \qquad (71)$$

$$\varphi_\nu^*{}_w' = \varphi_{\nu w}' - \frac{ic_i}{U_0'}\omega_{\nu w}'$$

For the binomial velocity distribution $U = 1 - (a - y)^n$ the values of the additional functions ω_{ν_a} ω_{ν_w} and their derivatives $\omega_{\nu}'_a$, $\omega_{\nu}'_w$ are given by the equations

$$
\left.
\begin{aligned}
\omega_{1a} &= \sum_{\nu=0}^{\infty} g_\nu \\
\omega_{2a} &= \frac{1}{a - y_c}\left[\sum_{\nu=1}^{\infty} h_\nu + \frac{2e_1\varphi_{1a}}{a - y_c}\right] \\
\omega_{1a}' &= \frac{1}{a - y_c}\sum_{\nu=1}^{\infty} \nu g_\nu \\
\omega_{2a}' &= \frac{1}{(a - y_c)^2}\sum_{\nu=1}^{\infty} \nu h_\nu + \frac{2e_1}{(a - y_c)^2}\left(-\frac{2\varphi_{1a}}{a - y_c} + \varphi_{1a}' + \omega_{1a}\right) \\
\omega_{1w} &= \sum_{\nu=0}^{\infty} g_\nu y_{1w}^{\nu} \\
\omega_{2w} &= \frac{1}{a - y_c}\left[\sum_{\nu=1}^{\infty} h_\nu y_{1w}^{\nu} + \frac{2e_1\varphi_{1w}}{a - y_c}\left(\frac{1}{y_{1w}} - \ln\left|y_{1w}\right|\omega_{1w}\right) + \right. \\
&\qquad \left. 2e_1 \ln\left|y_{1w}\right|\omega_{1w}\right] + i\pi\frac{U_0''}{U_0'}\left(\frac{\varphi_{1w}}{a - y_c} - \omega_{1w}\right) \\
\omega_{1w}' &= \frac{1}{a - y_c}\sum_{\nu=1}^{\infty} \nu g_\nu y_{1w}^{\nu-1} \\
\omega_{2w}' &= \frac{1}{(a - y_c)^2}\sum_{\nu=1}^{\infty} \nu h_\nu y_{1w}^{\nu-1} + \frac{2e_1}{(a - y_c)^2}\left[\frac{\varphi_{1w}}{a - y_c}\left(-\frac{1}{y_{1w}^2} - \frac{1}{y_{1w}}\right) + \right. \\
&\qquad \left. \varphi_{1w}'\left(\frac{1}{y_{1w}} - \ln\left|y_{1w}\right|\right) + \frac{\omega_{1w}}{y_{1w}} + \ln\left|y_{1w}\right|\omega_{1w}'(a - y_c)\right] + \\
&\qquad i\pi\frac{U_0''}{U_0'}\left(\frac{\varphi_{1w}'}{a - y_c} - \omega_{1w}'\right)
\end{aligned}
\right\} \quad (72)
$$

For the sinusoidal velocity distribution

$$U = U_s + (1 - U_s)\sin\left(\frac{y - s}{a - s}\frac{\pi}{2}\right)$$

in contrast, the corresponding formulas read

$$\left.\begin{aligned}
\omega_{1a} &= \sum_{\nu=0}^{\infty} g_\nu y_{2a}{}^\nu \\
\omega_{2a} &= \frac{\pi}{2(a-s)}\left[\sum_{\nu=1}^{\infty} h_\nu y_{2a}{}^\nu + \frac{\pi e_1 \varphi_{1a}}{a-s}\left(\frac{1}{y_{2a}} + \frac{\ln y_{2a}}{\sin y_{2s}\cos y_{2s}}\right) + 2e_1 \ln y_{2a}\omega_{1a}\right] \\
\omega_{1a}' &= \frac{\pi}{2(a-s)}\sum_{\nu=1}^{\infty} \nu g_\nu y_{2a}{}^{\nu-1} \\
\omega_{2a}' &= \frac{\pi^2}{4(a-s)^2}\sum_{\nu=1}^{\infty} \nu h_\nu y_{2a}{}^{\nu-1} + \frac{\pi^2 e_1}{2(a-s)^2}\left[\frac{\pi\varphi_{1a}}{2(a-s)}\left(-\frac{1}{y_{2a}{}^2} + \frac{1}{y_{2a}\sin y_{2s}\cos y_{2s}}\right) + \varphi_{1a}'\left(\frac{1}{y_{2a}} + \frac{\ln y_{2a}}{\sin y_{2s}\cos y_{2s}}\right) + \frac{\omega_{1a}}{y_{2a}}\frac{2(a-s)}{\pi} + \ln y_{2a}\omega_{1a}'\right] \\
\omega_{1w} &= \sum_{\nu=0}^{\infty} g_\nu y_{2w}{}^\nu \\
\omega_{2w} &= \frac{\pi}{2(a-s)}\left[\sum_{\nu=1}^{\infty} h_\nu y_{2w}{}^\nu + \frac{\pi e_1 \varphi_{1w}}{a-s}\left(\frac{1}{y_{2w}} + \frac{\ln|y_{2w}|}{\sin y_{2s}\cos y_{2s}}\right) + 2e_1 \ln|y_{2w}|\omega_{1w}\right] + i\pi\frac{U_0''}{U_0'}\left(\frac{-\pi\varphi_{1w}}{2(a-s)\sin y_{2s}\cos y_{2s}} - \omega_{1w}\right) \\
\omega_{1w}' &= \frac{\pi}{2(a-s)}\sum_{\nu=0}^{\infty} \nu g_\nu y_{2w}{}^{\nu-1} \\
\omega_{2w}' &= \frac{\pi^2}{4(a-s)^2}\sum_{\nu=1}^{\infty} \nu h_\nu y_{2w}{}^{\nu-1} + \frac{\pi^2 e_1}{2(a-s)^2}\left[\frac{\pi\varphi_{1w}}{2(a-s)}\left(-\frac{1}{y_{2w}{}^2} + \frac{1}{y_{2w}\sin y_{2s}\cos y_{2s}}\right) + \varphi_{1w}'\left(\frac{1}{y_{2w}} + \frac{\ln|y_{2w}|}{\sin y_{2s}\cos y_{2s}}\right) + \frac{\omega_{1w}}{y_{2w}} + \frac{2(a-s)}{\pi}\ln|y_{2w}|\omega_{1w}'\right] + i\pi\frac{U_0''}{U_0'}\left(\frac{-\pi\varphi_{1w}'}{2(a-s)\sin y_{2s}\cos y_{2s}} - \omega_{1w}'\right)
\end{aligned}\right\} \quad (73)$$

If the critical point shifts to the inflection point of the velocity distribution $\left(y_c = s,\ y_{2s} = 0\right)$, the equations for ω_{2a}, ω_{2a}', ω_{2w}, ω_{2w}' (equation (74)) are simplified to

$$\left.\begin{aligned}
\omega_{2a} &= \frac{\pi}{2(a-s)}\left[\sum_{\nu=1}^{\infty} h_\nu y_{2a}{}^\nu + \frac{\pi\varphi_{1a}}{2(a-s)} \ln y_{2a}\right] \\
\omega_{2a}' &= \frac{\pi^2}{4(a-s)^2}\left[\sum_{\nu=1}^{\infty} \nu h_\nu y_{2a}{}^{\nu-1} + \frac{\pi\varphi_{1a}}{2(a-s)y_{2a}} + \varphi_{1a}' \ln y_{2a}\right] \\
\omega_{2w} &= \frac{\pi}{2(a-s)}\left[\sum_{\nu=1}^{\infty} h_\nu y_{2w}{}^\nu + \frac{\pi\varphi_{1w}}{2(a-s)} \ln |y_{2w}|\right] - \frac{i\pi^3\varphi_{1w}}{4(a-s)^2} \\
\omega_{2w}' &= \frac{\pi^2}{4(a-s)^2}\left[\sum_{\nu=1}^{\infty} \nu h_\nu y_{2w}{}^{\nu-1} + \frac{\pi\varphi_{1w}}{2(a-s)y_{2w}} + \varphi_{1w}' \ln |y_{2w}|\right] - \\
&\quad \frac{i\pi^3\varphi_{1w}'}{4(a-s)^2}
\end{aligned}\right\} \quad (74)$$

We now split φ_{2w}, φ_{2w}', ω_{2w}, ω_{2w}' into real and imaginary parts according to the formulas

$$\left.\begin{aligned}
\varphi_{2w} &= A_1 + iB_1 \qquad \omega_{2w} = M_1 + iN_1 \\
\varphi_{2w}' &= A_2 + iB_2 \qquad \omega_{2w}' = M_2 + iN_2
\end{aligned}\right\} \quad (75)$$

then one obtains

$$\left.\begin{aligned}
\varphi_2{}^*{}_w &= A_1 + \frac{c_i}{U_0'} N_1 + i\left(B_1 - \frac{c_i}{U_0'} M_1\right) \\
\varphi_2{}^*{}_w' &= A_2 + \frac{c_i}{U_0'} N_2 + i\left(B_2 - \frac{c_i}{U_0'} M_2\right)
\end{aligned}\right\} \quad (76)$$

Then we put the expression (64) into the form

$$E^*(\alpha,c_r,c_i) = E(\alpha,c_r)\left[1 + c_i(z_1 + iz_2)\right] \tag{77}$$

where E, as previously defined in reference 1, is defined by

$$E = -\frac{1}{y_c}\frac{\varphi_{2w}\Phi_{1a} - \varphi_{1w}\Phi_{2a}}{\varphi_{2w}'\Phi_{1a} - \varphi_{1w}'\Phi_{2a}} \tag{78}$$

First, limiting oneself to the terms linear in c_i one has

$$\left.\begin{aligned}
\varphi_2^*{}_w\Phi_1^*{}_a &\sim A_1\Phi_{1a} + \frac{c_i}{U_0'}\left(N_1\Phi_{1a} + B_1\Omega_{1a}\right) + \\
&\qquad i\left[B_1\Phi_{1a} - \frac{c_i}{U_0'}\left(A_1\Omega_{1a} + M_1\Phi_{1a}\right)\right] \\
\varphi_1^*{}_w\Phi_2^*{}_a &\sim \varphi_{1w}\Phi_{2a} - \frac{ic_i}{U_0'}\left(\omega_{1w}\Phi_{2a} + \varphi_{1w}\Omega_{2a}\right) \\
\varphi_2^*{}_w'\Phi_1^*{}_a &\sim A_2\Phi_{1a} + \frac{c_i}{U_0'}\left(N_2\Phi_{1a} + B_2\Omega_{1a}\right) + \\
&\qquad i\left[B_2\Phi_{1a} - \frac{c_i}{U_0'}\left(A_2\Omega_{1a} + M_2\Phi_{1a}\right)\right] \\
\varphi_1^*{}_w'\Phi_2^*{}_a &\sim \varphi_{1w}'\Phi_{2a} - \frac{ic_i}{U_0'}\left(\omega_{1w}'\Phi_{2a} + \varphi_{1w}'\Omega_{2a}\right)
\end{aligned}\right\} \tag{79}$$

Hence, there results after a short intermediate calculation

$$E^* \sim E\left[1 - \frac{ic_i}{U_0' y_c} + \frac{c_i}{U_0'}\left\{\frac{(N_1\Phi_{1a} + B_1\Omega_{1a}) + i(\omega_{1w}\Phi_{2a} + \varphi_{1w}\Omega_{2a} - A_1\Omega_{1a} - M_1\Phi_{1a})}{A_1\Phi_{1a} - \varphi_{1w}\Phi_{2a} + iB_1\Phi_{1a}} - \frac{(N_2\Phi_{1a} + B_2\Omega_{1a}) + i(\omega_{1w}'\Phi_{2a} + \varphi_{1w}'\Omega_{2a} - A_2\Omega_{1a} - M_2\Phi_{1a})}{A_2\Phi_{1a} - \varphi_{1w}'\Phi_{2a} + iB_2\Phi_{1a}}\right\}\right] \tag{80}$$

We put for abbreviation

$$\left.\begin{aligned} N_1\Phi_{1a} + B_1\Omega_{1a} &= m_1 \\ \omega_{1w}\Phi_{2a} + \varphi_{1w}\Omega_{2a} - A_1\Omega_{1a} - M_1\Phi_{1a} &= n_1 \\ N_2\Phi_{1a} + B_2\Omega_{1a} &= m_2 \\ \omega_{1w}'\Phi_{2a} + \varphi_{1w}'\Omega_{2a} - A_2\Omega_{1a} - M_2\Phi_{1a} &= n_2 \\ A_1\Phi_{1a} - \varphi_{1w}\Phi_{2a} &= K_1 \\ A_2\Phi_{1a} - \varphi_{1w}'\Phi_{2a} &= K_2 \end{aligned}\right\} \tag{81}$$

Then there follows from equation (80)

$$E^* \sim E\left[1 - \frac{ic_i}{U_0'y_c} + \frac{c_i}{U_0'}\left\{\frac{m_1 + in_1}{K_1 + iB_1\Phi_{1a}} - \frac{m_2 + in_2}{K_2 + iB_2\Phi_{1a}}\right\}\right]$$

$$= E\left[1 - \frac{ic_i}{U_0'y_c} + \frac{c_i}{U_0'}\left\{\frac{m_1K_1 + n_1B_1\Phi_{1a}}{K_1^2 + B_1^2\Phi_{1a}^2} - \frac{m_2K_2 + n_2B_2\Phi_{1a}}{K_2^2 + B_2^2\Phi_{1a}^2}\right\} + \frac{ic_i}{U_0'}\left\{\frac{n_1K_1 - m_1B_1\Phi_{1a}}{K_1^2 + B_1^2\Phi_{1a}^2} - \frac{n_2K_2 - m_2B_2\Phi_{1a}}{K_2^2 + B_2^2\Phi_{1a}^2}\right\}\right] \tag{82}$$

If we finally introduce the designations

$$z_1 = \frac{1}{U_0'}\left[\frac{m_1K_1 + n_1B_1\Phi_{1a}}{K_1^2 + B_1^2\Phi_{1a}^2} - \frac{m_2K_2 + n_2B_2\Phi_{1a}}{K_2^2 + B_2^2\Phi_{1a}^2}\right]$$

$$z_2 = -\frac{1}{U_0'y_c} + \frac{1}{U_0'}\left[\frac{n_1K_1 - m_1B_1\Phi_{1a}}{K_1^2 + B_1^2\Phi_{1a}^2} - \frac{n_2K_2 - m_2B_2\Phi_{1a}}{K_2^2 + B_2^2\Phi_{1a}^2}\right] \tag{83}$$

the representation (77) is attained.

By means of the equations (70), (77), and (83) we thus have divided the two functions F^* and E^* (α, c_r, c_i) appearing in equation (65) into real and imaginary parts and can now graphically solve this equation. For this purpose, we plot for constant c_i for several values y_c the imaginary part of the function F^*

$$\underline{I}\left(F^*\right) = \underline{I}\left[F\left(\eta_0\right)\right] + \eta_0 \frac{c_i}{U_0'y_c}\left(1 + \frac{y_c}{3}\frac{U_0''}{U_0'}\right)\frac{dF_r}{d\eta_0} \tag{84}$$

against its real part

$$\underline{R}\left(F^*\right) = \underline{R}\left[F\left(\eta_0\right)\right] - \eta_0 \frac{c_i}{U_0'y_c}\left(1 + \frac{y_c}{3}\frac{U_0''}{U_0'}\right)\frac{dF_i}{d\eta_0} \tag{85}$$

and plot in this polar diagram to the same values c_i and y_c, the imaginary part of the function $E^*(\alpha,c_r,c_i)$

$$\underline{I}\left(E^*\right) = \underline{I}(E)(1 + c_i z_1) + c_i z_2 \underline{R}(E) \tag{86}$$

against its real part

$$\underline{R}\left(E^*\right) = \underline{R}(E)(1 + c_i z_1) - c_i z_2 \underline{I}(E) \tag{87}$$

The points of intersection of the functions F^* and E^* connected one to the other by the same pairs of values c_r, c_i yield first the values η_0 pertaining to the corresponding α-values, and then with (68) the curve $\alpha(Re^*)$ of the constant excitation c_i. This plotting and calculation then are repeated for other values c_i.

VI. RESULTS OF THE CALCULATION

As immediate result of the rather extensive calculations, the polar diagrams with the curves $E^*(\alpha,c_i,c_r)$ and $F^* = F(\eta_0^*)$ for several Hartree velocity distributions $U(y)$ in the laminar boundary layer are represented in figures 2 to 21. These boundary-layer profiles belong to the special class of pressure distributions

$$U_a = \text{const. } x^m \tag{88}$$

and are rigorous solutions of Prandtl's boundary-layer equations which were obtained with the aid of a Bush apparatus (ref. 6). We use, according to Hartree, for characterization of these boundary-layer profiles the parameter

$$\beta = \frac{2m}{1 + m} \tag{89}$$

The profiles with $m > 0$, $\beta > 0$ occur in case of decreasing pressure; the profiles with $m < 0$, $\beta < 0$ in case of increasing pressure. The profile $\beta = 1$ is the exact Hiemenz profile at the stagnation point of a cylindrical body, the profile $\beta = 0$ is the exact Blasius profile at the flat plate in longitudinal flow, and the profile $\beta = -0.198$ is a separation profile (wall shearing stress zero).

We have investigated the excitation for the Hartree profiles $\beta = 1, 0.6, 0.2, 0, -0.10, -0.198$ (the last, however, only for larger values of the Reynolds number, because of the uncertainty in case of small Re^*); as in an earlier report (ref. 3), we replaced them by binomial approximation distributions in case of decreasing pressure and by sinusoidal approximation distributions in case of increasing pressure, with the aid of the formulas

$$\left.\begin{array}{lll}
\beta = 1 & U = 1 - \left(1 - \frac{y}{a}\right)^4 & \frac{y}{a} = 0.3082\zeta \quad \zeta_a = 3.245 \\
\beta = 0.6 & U = 1 - \left(1 - \frac{y}{a}\right)^3 & \frac{y}{a} = 0.332\zeta \quad \zeta_a = 3.01 \\
\beta = 0.2 & U = 1 - \left(1 - \frac{y}{a}\right)^2 & \frac{y}{a} = 0.343\zeta \quad \zeta_a = 2.916 \\
\beta = 0 & U = \sin \frac{\pi}{2} \frac{y}{a} & \frac{y}{a} = 0.299\zeta \quad \zeta_a = 3.345 \\
\beta = -0.10 & U = 0.41 + 0.59 \sin \frac{\pi}{2 \times 0.6715}\left(\frac{y}{a} - 0.3285\right) & \frac{y}{a} = 0.274\zeta \quad \zeta_a = 3.65 \\
\beta = -0.198 & U = 0.5 + 0.5 \sin \pi\left(\frac{y}{a} - 0.5\right) & \frac{y}{a} = 0.2135\zeta \quad \zeta_a = 4.68
\end{array}\right\} \quad (90)$$

where

$$\zeta = y\sqrt{\frac{1}{2 - \beta} \frac{U_a}{\nu x}} \quad (91)$$

is the dimensionless wall distance used by Hartree and the coordinate a of the point of junction to the potential velocity U_a is connected with the displacement thickness by the relation

$$\frac{a}{\delta^*} = \frac{\zeta_a\sqrt{2 - \beta}}{k_\delta^*} \tag{92}$$

the quantity $k_\delta^*(\beta)$ may be found plotted graphically in figure 2 of reference 3.

The wall distance ζ_c of the critical layer indicated in figures 2 to 21 is obtained if in equation (91) y is replaced by y_c.

The following basic remarks should be made concerning the graphic solution of the eigenvalue problem in figures 2 to 21:

Since c_i has been presupposed so small that only the variations of the particular solutions φ_ν^* linear in c_i need to be taken into consideration compared to the solutions φ_ν for $c_i = 0$, the curves E^* and F^* appear for equal c_i-interval as "equidistant" curve families in the sense of equations (77) and (70). Actually, this "equidistance" will be lost in case of higher values of c_i; however, the calculation expenditure would increase intolerably even if only, for instance, the terms quadratic in c_i were to be taken into consideration. In this sense, the curves

$$\frac{\beta_i\delta^*}{U_a} = \frac{c_i\alpha\delta^*}{U_a}$$

against $\alpha\delta^*$ represented in figures 22 to 26 (from now on we use dimensional quantities) which result from the evaluation of the polar diagrams also are to be interpreted as approximations (in this and the following figures, the value β_i which is, according to equation (1), physically more important and which characterizes the logarithmic increment of the excited perturbation amplitude has been plotted instead of c_i). Here, as in Schlichting's report (ref. 4) mentioned before, only the derivative

$$\frac{d}{d(\alpha\delta^*)}\left(\frac{\beta_i\delta^*}{U_a}\right)$$

at the location $\frac{\beta_i \delta^*}{U_a} = 0$, that is, the slope of the $\frac{\beta_i \delta^*}{U_a}$ curve at the $\alpha\delta^*$-axis is rigorously correct. H. Schlichting interpolated between the base points at which he had determined the slope directly, although with a much higher calculation expenditure, with a curve of the third degree

$$\frac{\beta_i \delta^*}{U_a} = a_0 + a_1(\alpha\delta^*) + a_2(\alpha\delta^*)^2 + a_3(\alpha\delta^*)^3$$

where the four constants are fixed by the coordinates of the base points and the values of the curve slope in them. Thereby, Schlichting obtained for the Blasius profile higher values $\frac{\beta_i \delta^*}{U_a}$ than those occurring in figure 25 whereas the values of the slope are in agreement. Actually, the curves $\frac{\beta_i \delta^*}{U_a}(\alpha\delta^*)$ in the center part of the $(\alpha\delta^*)$-region enclosed in each case will run somewhat higher or lower than indicated by figures 22 to 26. At any rate, however, they may be interpreted as a first approximation in the usual sense.

These curves $\frac{\beta_i \delta^*}{U_a}$ over $\alpha\delta^*$ represent sections through the "excitation mountain range" enclosed by the neutral curve as base curve, along the lines $y_c = \text{Const.}$ or $c_r = \text{Const.}$ By interpolation one obtains from them the maps of excitation represented in figures 27 to 32, in which the lines of equal excitation $\frac{\beta_i \delta^*}{U_a} = \text{Const.}$, can be interpreted as "contour lines" of the "excitation mountain range." Instead of the lines of intersection $c_r = \text{Const.}$, we plotted in figures 27 to 32 the lines

$$\frac{\beta_r \nu}{U_a^2} = \frac{c_r \alpha\delta^*}{U_a \mathrm{Re}^*} = \text{Const.}$$

the significance of which will be discussed later in section VII. Even at first consideration of these excitation maps, a fundamental difference in the shape of the excitation mountain range is conspicuous according to whether the velocity profiles of the laminar friction layer lie in the region of decreasing pressure ($\beta > 0$) or of increasing pressure ($\beta < 0$).

In the region of decreasing pressure, the "excitation mountain range" has the form of a mountain with pronounced peak which is steeply ascending for a small Reynolds number Re^*, slowly flattens after a larger Re^* and shrinks to zero width and height for $\mathrm{Re}^* \rightarrow \infty$. The absolute height of the peak, that is, the maximum excitation increases with decreasing β.

In the region of increasing pressure, in contrast, the excitation mountain range changes behind the peak with growing Re^* into a "mountain ridge" of constant width and constant contour profile.

The properties of this "ridge" have been thoroughly investigated by W. Tollmien (ref. 5). Since we made use of Tollmien's theory, we must now briefly represent its results.

Searching for a general instability criterion, W. Tollmien established that the frictionless perturbation equation (5) possesses for the laminar velocity profiles in the region of pressure increase - which have a point of inflection in contrast to those of the region of decreasing pressure - for $Re^* \rightarrow \infty$ aside from the neutral solution existing for all profiles with the parameters

$$\alpha = 0 \qquad c_r = 0 \qquad \varphi_{nI} = U \tag{93}$$

in addition, the neutral solution with the parameters

$$\alpha = \alpha_s \qquad c_r = U_s \qquad \varphi_{nII} = \varphi_s \tag{94}$$

the subscript s therein denotes the point of inflection.

W. Tollmien calculated the eigenvalue α_s and the eigenfunction φ_s for the sinusoidal velocity distribution (30) which we also used from the frictionless perturbation equation (5)

$$(\alpha a)_s = - p \cot p \qquad \frac{p}{\sin p} = \frac{\pi}{2\left(1 - \frac{s}{a}\right)} \tag{95}$$

$$\left.\begin{aligned} \varphi_s &= \frac{\sin p \frac{y}{a}}{\sin \frac{ps}{a}} && \left(0 < y < a\right) \\ \varphi_s &= \frac{\sin p}{\sin \frac{ps}{a}} e^{\alpha a\left(1 - \frac{y}{a}\right)} && \left(y > a\right) \end{aligned}\right\} \tag{96}$$

For this second neutral eigensolution, the phase velocity c_r therefore equals the velocity of the basic flow at the point of inflection U_s.

For the excitation β_i and the circular frequency β_r in the neighborhood of the neutral frequencies $\alpha\delta^* = 0$ and $\alpha\delta^* = (\alpha\delta^*)_s$, W. Tollmien has derived the following formulas

$$\alpha = 0: \quad \frac{\beta_i \delta^*}{U_a} = \pi \frac{U_w''}{U_w'^4} \frac{U_a^3}{\delta^{*2}} (\alpha\delta^*)^3, \quad \frac{\beta_r \nu}{U_a^2} \mathrm{Re}^* = \frac{U_a}{U_w' \delta^*} (\alpha\delta^*)^2 \tag{97}$$

where the subscript w signifies that the values have to be taken at the wall $y = 0$, and that

$$\alpha = \alpha_s: \quad \frac{\beta_i \delta^*}{U_a} = B\left[(\alpha\delta^*)^3 - (\alpha_s\delta^*)^2 \alpha\delta^*\right], \quad \frac{\beta_r \nu}{U_a^2} \mathrm{Re}^*$$

$$= \frac{U_s}{U_a} \alpha\delta^* - \frac{BE}{\pi} \frac{U_s'^2}{U_s'''} \left[(\alpha\delta^*)^3 - (\alpha_s\delta^*)^2 \alpha\delta^*\right] \tag{98}$$

with

$$B = \pi \frac{U_s'''}{U_s'^2} \frac{\int_0^\infty \varphi_s dy}{U_a \delta^{*2} \left[E^2 + \frac{\pi^2 U_s'''^2}{U_s'^4}\right]} \tag{99}$$

where

$$E = \lim_{\epsilon \to 0} \left[\int_0^{s-\epsilon} \frac{U''}{(U - U_s)^2} \varphi_s^2 dy + \int_{s+\epsilon}^\infty \frac{U''}{(U - U_s)^2} \varphi_s^2 dy\right] \tag{100}$$

We have calculated the "ridge contour profiles" of the excitation and the circular frequency according to the formulas (97) and (98) for the Hartree velocity distributions $\beta = -0.10$, -0.14, -0.16, -0.18, -0.198; the values for the derivatives of the velocity were not taken from the sinusoidal approximation distribution but from the exact velocity distribution. These "ridge contour profiles" of the excitation and the circular frequency have been plotted in figures 33 and 34. The curves corresponding to the formulas just mentioned have been drawn in solid lines; the transitions between the two curve arcs, interpolated somewhat arbitrarily, have been drawn in dashed lines. In the range

of very large Re^*, the lines of constant excitation and constant circular frequency were transferred from figures 33 and 34 into figures 31 and 32.

Figure 35 represents the variation of the maximum excitation

$$\left(\frac{\beta_i \delta^*}{U_a}\right)_{max}$$

against the form parameter β, separately for the excitation for finite Re^* (peak of the excitation mountain range) and for $Re^* > \infty$ (ridge of the excitation mountain range). For $\beta < -0.10$ these two values seem more and more to approach one another so that with decreasing β the peak becomes less and less pronounced, and the excitation starting from small Re^* monotonically increases to the values of the "ridge contour profile."

This figure and the preceding ones show clearly that the maximum excitation and accordingly the excitation in general is considerably larger in the region of pressure increase than in that of pressure decrease for smaller Re^* as well.

After thus having estimated the magnitude of excitation in the entire instability range of all velocity distributions occurring in the laminar friction layer, we shall discuss the physical conclusions resulting from our calculations for the position of the transition point.

VII. DISCUSSION OF THE RESULTS

Let the pressure distribution $U_a(x)$ against the arc length of the cross section profile, and the oscillation of circular time frequency β_r be prescribed. Then this oscillation superposed on the boundary-layer flow travels downstream on a curve

$$\frac{\beta_r \nu}{U_a^2} = f(x)$$

As we mentioned at the beginning, there pertains to every point x of the profile in the flow a fixed value of the Pohlhausen parameter λ which characterizes by way of approximation the velocity distribution in the boundary layer at this point. According to figure 34 in reference 3 one may coordinate to this parameter λ the Hartree parameter β

and therewith one of the excitation maps calculated in the present report (figs. 27 to 32). In order to obtain the excitation of the perturbation β_r at a certain point x of the profile, one has therefore to read off the excitation $\frac{\beta_i \delta^*}{U_a}$ (number of the "contour line") on the corresponding excitation map at the point of the map determined by the pair of values of the Reynolds number

$$Re^* = \frac{U_a \delta^*}{\nu} = g(x)$$

and the dimensionless circular frequency

$$\frac{\beta_r \nu}{U_a^2} = f(x)$$

We shall start the discussion of the results of our above excitation calculations with the limiting case of a small Reynolds number $Re = \frac{U_\infty t}{\nu}$. According to the explanations in section I (compare fig. 1) the stability limit lies, for small Reynolds numbers only, at the point where the laminar boundary layer separates. If the perturbation waves are so long that the curve

$$\frac{\beta_\nu \nu}{U_a^2} = f(x)$$

intersects the instability region for the separation profile ($\beta = -0.198$), it is very violently excited when entering this zone and leads quickly to transition to the turbulent flow pattern. The transition point then practically coincides with the separation point which we had denoted its rearward limit. If, on the other hand, the perturbation waves are very short so that the curve

$$\frac{\beta_r \nu}{U_a^2} = f(x)$$

does not intersect the instability region, the laminar layer separates without transition.

If the Reynolds number $Re = \frac{U_\infty t}{\nu}$ increases, the stability limit shifts forward in the direction toward the pressure minimum (fig. 1), the perturbation enters a region of instability further upstream for a larger value of the parameter β or the Pohlhausen parameter λ, and is there initially excited to a degree which decreases the more the stability limit shifts forward but which increases due to the fact that the perturbation downstream (with decreasing β or λ) reaches instability zones with rapidly increasing excitation. The transition point shifts frontward corresponding to the excitation which started earlier and is still strong.

If we finally increase the Reynolds number $Re = \frac{U_\infty t}{\nu}$ so that the stability limit shifts ahead of the pressure minimum, the excitation in turn starts accordingly sooner; however - and this must be regarded as the most important result of our calculations for the time being - in the region of decreasing pressure, the excitation is so slight that it generally attains amounts equalling the excitations produced in the cases treated just now only after having passed the pressure minimum.

In this manner, one may easily give the theoretical explanation for the fact proved by many experiments, that the transition point even in case of very high Reynolds numbers rarely ever shifts ahead of the pressure minimum. Only in cases of very long acceleration sections and perturbations with very long waves where the perturbation does not too soon leave the instability region again, the limited excitation of the region of decreasing pressure will be sufficient to induce the transition still in the region of pressure decrease. However, these cases are rare in technical application.

A detailed calculation of the degree of excitation which causes the transition is meaningful only in connection with corresponding experiments. Therefore, it will be postponed until these experiments, now in the preparatory stage, have been carried out. Probably one will have to regard the form of the pressure distribution in the region of pressure increase as the most important test condition since, according to our theoretical deliberations, the contributions to the excitation of perturbations in the region of pressure decrease are insignificant. The aim of this experimental investigation and of the excitation calculation to be performed simultaneously on the basis of the present report will be to find a connection between the pressure-distribution form and the degree of excitation attained at the measured transition point so that it will be possible to calculate, inversely, the transition point for a prescribed pressure distribution from this relation.

VIII. SUMMARY

As a contribution to the solution of the important problem of the calculation of the transition point of a plane laminar flow, we had first determined (in an earlier report, according to Tollmien's method of small oscillations for the Hartree velocity distributions appearing in the boundary layer in case of decreasing and of increasing pressure) only the critical Reynolds number beyond which the perturbations superposed on the laminar flow are excited. In connection with those calculations now, the excitation itself in the entire instability range of the perturbations was calculated. The excitation in the narrow instability range of decreasing pressure turns out to be very much smaller than the excitation in the more extensive instability range of increasing pressure; thus the known fact that the transition point generally does not shift ahead of the pressure minimum even in case of high Reynolds numbers may be explained on a theoretical basis, as shown in tables 1, 2, and 3.

Systematic experimental measurements of the transition point, together with calculations to be performed on the basis of the results given here, are to establish the connection between the variation of the pressure gradient and the degree of excitation which produces the transition and thereby a basis for determination of the transition point for prescribed pressure variation by calculation.

Translated by Mary L. Mahler
National Advisory Committee
for Aeronautics

REFERENCES

1. Tollmien, W.: Über die Entstenhung der Turbulenz. Nachr. d. Ges. d. Wiss. zw Göttingen Math.-Phys. Kl., 1929, pp. 21-44. (Available as NACA TM 609.)

2. Schlichting, H., and Bussmann, K.: Zur Berechnung des Umschlages laminar = turbulent (Preisausschreiben 1940 der Lilienthal-Gesellschaft für Luftfahrtforschung), dieses Jahrbuch.

3. Pretsch, J.: Die Stabilität einer ebenen Laminarströmung bei Druckgefälle und Druckanstieg (Preisausschreiben 1940 der Lilienthal-Gesellschaft für Luftfahrtforschung). Jahrbuch 1941 der Deutschen Luftfahrtforschung, p. 58.

4. Schlichting, H.: Zur Entstehung der Turbulenz bei der Plattenstromung. Nachr. Ges. Wiss. Göttingen Math. Phys. Klasse, 1933, pp. 181-208.

5. Tollmien, W.: Ein allgemeneines Kriterium der Instabilität laminarer Geschwindigkeitsverteilungen. Nachr. d. Ges. d. Wiss. zw Göttingen, Math.-Phys. Kl., Neue Folge, Vol. 1, No. 5, 1935, pp. 79-114. (Available as NACA TM 792.)

6. Hartree, D. R.: On an Equation Occurring in Falkner and Skan's Approximate Treatment of the Equation of the Boundary Layer. Proc. Phil. Soc. Cambridge, Vol. 33, 1937, pp. 223-239.

TABLE 1

SERIES COEFFICIENTS OF THE SOLUTIONS φ_1^*, φ_2^* FOR THE BASIC FLOW

$U = 1 - (a - y)^n$; $n = 1, 2, 3, 4$

n = 1

$$\bar{y} = \frac{y - y_c}{y_c} \qquad \bar{y}^* = \frac{y - y_c^*}{y_c} \qquad \bar{\alpha} = \alpha y_c$$

$$\varphi_1^* = \frac{1}{\bar{\alpha}} \sin\left(\bar{\alpha}\,\bar{y}^*\right) \approx \frac{1}{\bar{\alpha}} \sin\left[\bar{\alpha}\left(\bar{y} - \frac{ic_1}{u_0' y_c}\right)\right] \approx \varphi_1 - \frac{ic_1}{u_0'} \cos\left(\bar{\alpha}\,\bar{y}\right) = \varphi_1 - \frac{ic_1}{u_0'}\,\varphi_2$$

$$\varphi_2^* = \cos\left(\bar{\alpha}\,\bar{y}^*\right) \approx \cos\left[\bar{\alpha}\left(\bar{y} - \frac{ic_1}{u_0' y_c}\right)\right] \approx \varphi_2 - \frac{ic_1\alpha}{u_0'} \sin\left(\bar{\alpha}\,\bar{y}\right) = \varphi_2 - \frac{ic_1\alpha^2}{u_0'}\,\varphi_1$$

n = 2

$$\beta_0^* = 0 \qquad \beta_1^* = 1 - if_1 \qquad \beta_2^* = -\frac{1}{2}(1 - if_1) - \alpha_1^2 \qquad \beta_\nu^* = \frac{1}{2^{\nu-1}}(1 - i\nu f_1) \qquad (\nu \geq 3)$$

$$e_0^* = 1 \qquad e_1^* = -\frac{1}{2}(1 - if_1)$$

$$e_2^* = +\frac{\alpha_1^2}{6} \qquad e_3^* = -\frac{\alpha_1^2}{18}(1 - if_1)$$

$$e_4^* = -\frac{\alpha_1^2}{720}(1 - 2if_1) + \frac{\alpha_1^4}{120} \qquad e_5^* = -\frac{\alpha_1^2}{2400}(1 - 3if_1) - \frac{23\alpha_1^4}{10800}(1 - if_1)$$

$$e_6^* = -\frac{\alpha_1^2}{7200}(1 - 4if_1) - \frac{37\alpha_1^4}{453600}(1 - 2if_1) + \frac{\alpha_1^6}{5040} \qquad e_7^* = -\frac{\alpha_1^2}{20160}(1 - 5if_1) - \frac{59\alpha_1^4}{6350400}(1 - 3if_1) - \frac{11\alpha_1^6}{264600}(1 - if_1)$$

. . . . .

$$b_2^* = -(1 - 2if_1) + \frac{\alpha_1^2}{2} \qquad b_3^* = \frac{1}{8}(1 - 3if_1) + \frac{\alpha_1^2}{18}(1 - if_1)$$

$$b_4^* = \frac{1}{48}(1 - 4if_1) - \frac{61\alpha_1^2}{432}(1 - 2if_1) + \frac{\alpha_1^4}{24} \qquad b_5^* = \frac{1}{192}(1 - 5if_1) + \frac{109\alpha_1^2}{21600}(1 - 3if_1) + \frac{\alpha_1^4}{225}(1 - if_1)$$

$$b_6^* = \frac{1}{640}(1 - 6if_1) + \frac{13\alpha_1^2}{72000}(1 - 4if_1) - \frac{2051\alpha_1^4}{324000}(1 - 2if_1) + \frac{\alpha_1^6}{720}$$

$$b_7^* = \frac{1}{1920}(1 - 7if_1) - \frac{79\alpha_1^2}{1512000}(1 - 5if_1) - \frac{439\alpha_1^4}{7938000}(1 - 3if_1) + \frac{71\alpha^6}{529200}(1 - if_1)$$

. . . . .

$$g_0 = 1 \qquad g_1 = -1$$

$$g_2 = \frac{1}{2} + \frac{\alpha_1^2}{2} \qquad g_3 = -\frac{2}{9}\alpha_1^2$$

$$g_4 = \frac{7}{144}\alpha_1^2 + \frac{1}{24}\alpha_1^4 \qquad g_5 = \frac{1}{3600}\alpha_1^2 - \frac{23\alpha_1^4}{1800}$$

$$g_6 = \frac{1}{3600}\alpha_1^2 + \frac{101}{64800}\alpha_1^4 + \frac{\alpha_1^6}{720} \qquad g_7 = \frac{1}{6300}\alpha_1^2 + \frac{141}{1587600}\alpha_1^4 - \frac{11\alpha_1^6}{33075}$$

. . . . .

$$h_0 = 0 \qquad h_1 = -2 + \alpha_1^2$$

$$h_2 = \frac{19}{8} + \frac{\alpha_1^2}{6} \qquad h_3 = -\frac{7}{24} - \frac{67}{108}\alpha_1^2 + \frac{\alpha_1^4}{6}$$

$$h_4 = -\frac{11}{192} + \frac{443}{1440}\alpha_1^2 + \frac{\alpha_1^4}{45} \qquad h_5 = -\frac{1}{60} - \frac{5411}{360000}\alpha_1^2 - \frac{2291}{54000}\alpha_1^4 + \frac{\alpha_1^6}{120}$$

$$h_6 = -\frac{11}{1920} - \frac{47}{43200}\alpha_1^2 + \frac{6959}{567000}\alpha_1^4 + \frac{71}{75600}\alpha_1^6$$

. . . . .

TABLE 1

SERIES COEFFICIENTS OF THE SOLUTIONS φ_1^*, φ_2^* FOR THE BASIC FLOW

$U = 1 - (a + y)^n$; $n = 1, 2, 3, 4$ - Continued

$n = 3$

$\beta_0^* = 0$

$\beta_1^* = 2(1 - if_1)$

$\beta_2^* = -\alpha_1^2$

$\beta_{3+6v}^* = (-1)^{v+1} \frac{2}{3^{1+3v}}\left[1 - (3 + 6v)if_1\right]$

$\beta_{4+6v}^* = (-1)^{v+1} \frac{2}{3^{1+3v}}\left[1 - (4 + 6v)if_1\right]$

$\beta_{5+6v}^* = (-1)^{v+1} \frac{4}{3^{2+3v}}\left[1 - (5 + 6v)if_1\right]$

$\beta_{6+6v}^* = (-1)^{v+1} \frac{2}{3^{2+3v}}\left[1 - (6 + 6v)if_1\right]$

$\beta_{7+6v}^* = (-1)^{v+1} \frac{2}{3^{3+3v}}\left[1 - (7 + 6v)if_1\right]$

$\beta_{8+6v}^* = 0; \quad v = 0,1,2, \ldots$

$e_0^* = 1$

$e_1^* = -(1 - if_1)$

$e_2^* = \frac{1}{3}(1 - 2if_1) + \frac{\alpha_1^2}{6}$

$e_3^* = -\frac{\alpha_1^2}{9}(1 - if_1)$

$e_4^* = \frac{\alpha_1^2}{36}(1 - 2if_1) + \frac{\alpha_1^4}{120}$

$e_5^* = \frac{\alpha_1^2}{540}(1 - 3if_1) - \frac{23\alpha_1^4}{5400}(1 - if_1)$

$e_6^* = \frac{\alpha_1^2}{1260}(1 - 4if_1) + \frac{7\alpha_1^2}{8100}(1 - 2if_1) + \frac{\alpha_1^6}{5040}$

$e_7^* = \frac{2\alpha_1^2}{6615}(1 - 5if_1) + \frac{23\alpha_1^4}{226800}(1 - 3if_1) - \frac{11\alpha_1^6}{132300}(1 - if_1)$

$e_8^* = \frac{\alpha_1^2}{10584}(1 - 6if_1) + \frac{5\alpha_1^4}{108864}(1 - 4if_1) + \frac{409\alpha_1^6}{28576800}(1 - 2if_1) + \frac{\alpha_1^8}{362880}$

. . . . .

$b_2^* = -3(1 - 2if_1) + \frac{\alpha_1^2}{2}$

$b_3^* = \frac{2}{3}(1 - 3if_1) + \frac{\alpha_1^2}{9}(1 - if_1)$

$b_4^* = -\frac{2}{9}(1 - 4if_1) - \frac{43}{108}\alpha_1^2(1 - 2if_1) + \frac{\alpha_1^4}{24}$

$b_5^* = -\frac{1}{18}(1 - 5if_1) + \frac{89}{540}\alpha_1^2(1 - 3if_1) + \frac{2}{225}\alpha_1^4(1 - if_1)$

$b_6^* = -\frac{1}{54}(1 - 6if_1) - \frac{1549}{14175}\alpha_1^2(1 - 4if_1) - \frac{172}{10125}\alpha_1^4(1 - 2if_1) + \frac{\alpha_1^6}{720}$

$b_7^* = -\frac{1}{162}(1 - 7if_1) - \frac{27973}{396900}\alpha_1^2(1 - 5if_1) + \frac{179\alpha_1^4}{31500}(1 - 3if_1) + \frac{71}{264600}\alpha_1^6(1 - if_1)$

$b_8^* = -\frac{1}{567}(1 - 8if_1) - \frac{21829}{617400}\alpha_1^2(1 - 6if_1) + \frac{93779}{13608000}(1 - 4if_1) - \frac{39727\alpha_1^6}{111132000}(1 - 2if_1) + \frac{\alpha_1^8}{40320}$

. . . . .

$g_0 = 1$

$g_1 = -2$

$g_2 = 2 + \frac{\alpha_1^2}{2}$

$g_3 = -\frac{2}{3} - \frac{4}{9}\alpha_1^2$

$g_4 = \frac{\alpha_1^2}{4} + \frac{\alpha_1^4}{24}$

$g_5 = -\frac{2}{45}\alpha_1^2 - \frac{23}{900}\alpha_1^4$

$g_6 = \frac{167}{16200}\alpha_1^4 + \frac{\alpha_1^6}{720}$

$g_7 = -\frac{\alpha_1^2}{1323} - \frac{13}{14175}\alpha_1^4 - \frac{22\alpha_1^6}{33075}$

$g_8 = -\frac{\alpha_1^2}{1512} + \frac{11}{100800}\alpha_1^4 + \frac{673\alpha_1^6}{3175200} + \frac{\alpha_1^8}{40320}$

. . . . .

$h_0 = 0$

$h_1 = -6 + \alpha_1^2$

$h_2 = 11 + \frac{\alpha_1^2}{3}$

$h_3 = -\frac{53}{9} - \frac{46}{27}\alpha_1^2 + \frac{\alpha_1^4}{6}$

$h_4 = \frac{11}{18} + \frac{175}{108}\alpha_1^2 + \frac{2}{45}\alpha_1^4$

$h_5 = \frac{1}{6} - \frac{21737\alpha_1^2}{18900} - \frac{374}{3375}\alpha_1^4 + \frac{\alpha_1^6}{120}$

$h_6 = \frac{11}{162} - \frac{1063}{18900}\alpha_1^2 + \frac{2987}{40500}\alpha_1^4 + \frac{71}{37800}\alpha_1^6$

$h_7 = \frac{11}{378} - \frac{193211\alpha_1^2}{2778300} + \frac{64781}{1701000}\alpha_1^4 - \frac{86909\alpha_1^6}{27783000} + \frac{\alpha_1^8}{5040}$

TABLE 1

SERIES COEFFICIENTS OF THE SOLUTIONS φ_1^*, φ_2^* FOR THE BASIC FLOW

$U = 1 - (a - y)^n$; n = 1, 2, 3, 4 - Concluded

n = 4

$\beta_0^* = 0$

$\beta_1^* = 3(1 - if_1)$

$\beta_2^* = -\frac{3}{2}(1 - 2if_1) - a_1^2$

$\beta_3^* = -\frac{9}{4}(1 - 3if_1)$

$\beta_4^* = -\frac{9}{8}(1 - 4if_1)$

$\beta_5^* = \frac{3}{16}(1 - 5if_1)$

$\beta_6^* = \frac{27}{32}(1 - 6if_1)$

$\beta_7^* = \frac{51}{64}(1 - 7if_1)$

$\beta_8^* = \frac{51}{128}(1 - 8if_1)$

$\beta_9^* = \frac{3}{256}(1 - 9if_1)$

$\beta_{10}^* = -\frac{93}{512}(1 - 10if_1)$

. . . . .

$e_0^* = 1$

$e_1^* = -\frac{3}{2}(1 - if_1)$

$e_2^* = (1 - 2if_1) + \frac{a_1^2}{6}$

$e_3^* = -\frac{1}{4}(1 - 3if_1) - \frac{a_1^2}{6}(1 - if_1)$

$e_4^* = \frac{7}{80}a_1^2(1 - 2if_1) + \frac{a_1^4}{120}$

$e_5^* = -\frac{31}{2400}a_1^2(1 - 3if_1) - \frac{23}{3600}a_1^4(1 - if_1)$

$e_6^* = -\frac{a_1^2}{2400}(1 - 4if_1) + \frac{143a_1^4}{50400}(1 - 2if_1) + \frac{a_1^6}{5040}$

$e_7^* = -\frac{a_1^2}{1400}(1 - 5if_1) - \frac{103a_1^4}{470400}(1 - 3if_1) - \frac{11a_1^6}{88200}(1 - if_1)$

$e_8^* = -\frac{431a_1^2}{2^9 \times 3^2 \times 5^2 \times 7}(1 - 6if_1) - \frac{79a_1^4}{2^{10} \times 3^2 \times 5^2 \times 7^2}(1 - 4if_1) + \frac{619a_1^6}{2^7 \times 3^4 \times 5^2 \times 7^2}(1 - 2if_1) + \frac{a_1^8}{2^7 \times 3^4 \times 5 \times 7}$

$e_9^* = -\frac{253a_1^2}{2^{10} \times 3^3 \times 5 \times 7}(1 - 7if_1) - \frac{12749a_1^4}{2^{11} \times 3^3 \times 5^3 \times 7^2}(1 - 5if_1) - \frac{a_1^6}{2^2 \times 3^5 \times 5^3 \times 7}(1 - 3if_1) - \frac{563a_1^8}{2^8 \times 3^5 \times 5^3 \times 7^2}(1 - if_1)$

. . . . .

$b_2^* = -6(1 - 2if_1) + \frac{a_1^2}{2}$

$b_3^* = \frac{47}{8}(1 - 3if_1) + \frac{a_1^2}{6}(1 - if_1)$

$b_4^* = -\frac{41}{16}(1 - 4if_1) - \frac{37a_1^2}{48}(1 - 2if_1) + \frac{a_1^4}{24}$

$b_5^* = \frac{9}{64}(1 - 5if_1) + \frac{477a_1^2}{800}(1 - 3if_1) + \frac{a_1^4}{75}(1 - if_1)$

$b_6^* = \frac{29}{640}(1 - 6if_1) - \frac{3997a_1^2}{24000}(1 - 4if_1) - \frac{1151a_1^4}{36000}(1 - 2if_1) + \frac{a_1^6}{720}$

$b_7^* = \frac{19}{640}(1 - 7if_1) - \frac{163a_1^2}{56000}(1 - 5if_1) + \frac{401a_1^4}{18375}(1 - 3if_1) + \frac{71a_1^6}{176400}(1 - if_1)$

$b_8^* = \frac{39}{2240}(1 - 8if_1) - \frac{11573a_1^2}{3136000}(1 - 6if_1) - \frac{1503559}{395136000}(1 - 4if_1) - \frac{32377a_1^6}{49392000}(1 - 2if_1) + \frac{a_1^8}{40320}$

. . . . .

$g_0 = 1$

$g_1 = -3$

$g_2 = \frac{9}{2} + \frac{a_1^2}{2}$

$g_3 = -3 - \frac{2}{3}a_1^2$

$g_4 = \frac{3}{4} + \frac{29}{48}a_1^2 + \frac{a_1^4}{24}$

$g_5 = -\frac{101}{400}a_1^2 - \frac{23}{600}a_1^4$

$g_6 = \frac{43}{1200}a_1^2 + \frac{21}{800}a_1^4 + \frac{a_1^6}{720}$

$g_7 = -\frac{17}{4200}a_1^2 - \frac{131a_1^4}{17640} - \frac{11a_1^6}{11025}$

$g_8 = -\frac{111}{89600}a_1^2 + \frac{149a_1^4}{250880} + \frac{159a_1^6}{282240} + \frac{a_1^8}{40320}$

. . . . .

$h_0 = 0$

$h_1 = -12 + a_1^2$

$h_2 = \frac{237}{8} + \frac{a_1^2}{2}$

$h_3 = -\frac{223}{8} - \frac{13}{4}a_1^2 + \frac{a_1^4}{6}$

$h_4 = \frac{701}{64} + \frac{2171}{480}a_1^2 + \frac{a_1^4}{15}$

$h_5 = -\frac{69}{160} - \frac{697}{250}a_1^2 - \frac{1231}{6000}a_1^4 + \frac{a_1^6}{120}$

$h_6 = -\frac{41}{640} + \frac{15499}{24000}a_1^2 + \frac{5461}{25200}a_1^4 + \frac{71}{25200}a_1^6$

$h_7 = -\frac{307}{4480} - \frac{1467}{98000}a_1^2 - \frac{4737223}{49392000}a_1^4 - \frac{17431}{3087000}a_1^6 + \frac{a_1^8}{5040}$

TABLE 2

SERIES COEFFICIENTS OF THE SOLUTIONS φ_1^*, φ_2^* FOR THE BASIC FLOW $U = U_s + (1 - U_s)\sin\left(\frac{y - s}{a - s}\frac{\pi}{2}\right)$. ABBREVIATION: $p = \frac{f_2}{\sin y_{2s}\cos y_{2s}}$

$$\beta_0^* = 0 \qquad \beta_1^* = -\tan y_{2s}(1 + ip) \qquad \beta_2^* = 1 + \tfrac{1}{2}\tan^2 y_{2s}(1 + 2ip) - \alpha_2^2$$

$$\beta_3^* = -\tfrac{1}{6}\tan y_{2s}(1 + ip) - \tfrac{1}{4}\tan^3 y_{2s}(1 + 3ip)$$

$$\beta_4^* = \tfrac{1}{8}\tan^2 y_{2s}(1 + 2ip) + \tfrac{1}{8}\tan^4 y_{2s}(1 + 4ip)$$

$$\beta_5^* = -\tfrac{7}{360}\tan y_{2s}(1 + ip) - \tfrac{1}{12}\tan^3 y_{2s}(1 + 3ip) - \tfrac{1}{16}\tan^5 y_{2s}(1 + 5ip)$$

$$\beta_6^* = \tfrac{1}{48}\tan^2 y_{2s}(1 + 2ip) + \tfrac{5}{96}\tan^4 y_{2s}(1 + 4ip) + \tfrac{1}{32}\tan^6 y_{2s}(1 - 6ip)$$

$$\beta_7^* = -\tfrac{31}{15120}\tan y_{2s}(1 + ip) - \tfrac{17}{960}\tan^3 y_{2s}(1 + 3ip) - \tfrac{1}{32}\tan^5 y_{2s}(1 + 5ip) - \tfrac{1}{64}\tan^7 y_{2s}(1 + 7ip)$$

$$\beta_8^* = \tfrac{17}{5760}\tan^2 y_{2s}(1 + 2ip) + \tfrac{77}{5760}\tan^4 y_{2s}(1 + 4ip) + \tfrac{7}{384}\tan^6 y_{2s}(1 + 6ip) + \tfrac{1}{128}\tan^8 y_{2s}(1 + 8ip)$$

$$e_0^* = 1 \qquad e_1^* = \tfrac{1}{2}\tan y_{2s}(1 + ip) \qquad e_2^* = -\tfrac{1}{6} + \tfrac{1}{6}\alpha_2^2$$

$$e_3^* = -\tfrac{1}{24}\tan y_{2s}(1 + ip) + \frac{\alpha_2^2}{18}\tan y_{2s}(1 + ip)$$

$$e_4^* = \tfrac{1}{120} - \frac{\alpha_2^2}{60}\left[1 + \tfrac{1}{12}\tan^2 y_{2s}(1 + 2ip)\right] + \frac{\alpha_2^4}{120}$$

$$e_5^* = \tfrac{1}{720}\tan y_{2s}(1 + ip) - \frac{\alpha_2^2}{1200}\left[\tfrac{31}{9}\tan y_{2s}(1 + ip) - \tfrac{1}{2}\tan^3 y_{2s}(1 + 3ip)\right] + \frac{23}{10800}\alpha_2^4\tan y_{2s}(1 - ip)$$

$$e_6^* = -\tfrac{1}{5040} + \frac{\alpha_2^2}{1680}\left[1 - \tfrac{17}{90}\tan^2 y_{2s}(1 + 2ip) - \tfrac{7}{30}\tan^4 y_{2s}(1 + 4ip)\right] - \frac{\alpha_2^4}{1680}\left[1 + \tfrac{37}{270}\tan^2 y_{2s}(1 + 2ip)\right] + \frac{\alpha_2^6}{5040}$$

$$e_7^* = -\tfrac{1}{40320}\tan y_{2s}(1 + ip) + \frac{\alpha_2^2}{6720}\left[\tfrac{67}{105}\tan y_{2s}(1 + ip) + \tfrac{29}{70}\tan^3 y_{2s}(1 + 3ip) + \tfrac{1}{3}\tan^5 y_{2s}(1 + 5ip)\right] -$$
$$\frac{\alpha_2^4}{50400}\left[\tfrac{53}{14}\tan y_{2s}(1 + ip) - \tfrac{307}{243}\tan^3 y_{2s}(1 + 3ip)\right] + \frac{11\alpha_2^6}{264600}\tan y_{2s}(1 + ip)$$

$$e_8^* = \tfrac{1}{362880} - \frac{\alpha_2^2}{10080}\left[\tfrac{1}{9} + \tfrac{619}{5040}\tan^2 y_{2s}(1 + 2ip) + \tfrac{257}{840}\tan^4 y_{2s}(1 + 4ip) + \tfrac{3}{16}\tan^6 y_{2s}(1 + 6ip)\right] +$$
$$\frac{\alpha_2^4}{60480}\left[1 - \tfrac{131}{315}\tan^2 y_{2s}(1 + 2ip) - \tfrac{14263}{29160}\tan^4 y_{2s}(1 + 4ip)\right] - \frac{\alpha_2^6}{90720}\left[1 + \tfrac{221}{1260}\tan^2 y_{2s}(1 + 2ip)\right] + \frac{\alpha_2^8}{362880}$$

$$b_2^* = -\left[\tfrac{1}{2} + \tan^2 y_{2s}(1 + 2ip)\right] + \tfrac{1}{2}\alpha_2^2$$

$$b_3^* = \left[\tfrac{1}{12}\tan y_{2s}(1 + ip) - \tfrac{1}{8}\tan^3 y_{2s}(1 + 3ip)\right] - \frac{\alpha_2^2}{18}\tan y_{2s}(1 + ip)$$

$$b_4^* = \left[\tfrac{1}{24} + \tfrac{1}{8}\tan^2 y_{2s}(1 + 2ip) + \tfrac{1}{48}\tan^4 y_{2s}(1 + 4ip)\right] - \alpha_2^2\left[\tfrac{1}{12} + \tfrac{61}{432}\tan^2 y_{2s}(1 + 2ip)\right] + \frac{\alpha_2^4}{24}$$

$$b_5^* = -\left[\tfrac{13}{1440}\tan y_{2s}(1 + ip) + \tfrac{1}{192}\tan^5 y_{2s}(1 + 5ip)\right] + \alpha_2^2\left[\tfrac{13}{900}\tan y_{2s}(1 + ip) - \tfrac{109}{21600}\tan^3 y_{2s}(1 + 3ip)\right] -$$
$$\frac{\alpha_2^4}{225}\tan y_{2s}(1 + ip)$$

$$b_6^* = \left[-\tfrac{1}{720} - \tfrac{11}{2880}\tan^2 y_{2s}(1 + 2ip) + \tfrac{1}{576}\tan^4 y_{2s}(1 + 4ip) + \tfrac{1}{640}\tan^6 y_{2s}(1 + 6ip)\right] +$$
$$\alpha_2^2\left[\tfrac{1}{240} + \tfrac{2051}{324000}\tan^2 y_{2s}(1 + 2ip)\right] + \frac{\alpha_2^6}{720}$$

$$b_7^* = \tfrac{41}{181440}\tan y_{2s}(1 + ip) - \tfrac{1}{1920}\tan^3 y_{2s}(1 + 3ip) - \tfrac{1}{1152}\tan^5 y_{2s}(1 + 5ip) - \tfrac{1}{1920}\tan^7 y_{2s}(1 + 7ip)$$
$$\alpha_2^2\left[-\tfrac{1573}{2116800}\tan y_{2s}(1 + ip) + \tfrac{4889}{15876000}\tan^3 y_{2s}(1 + 3ip) + \tfrac{79}{1512000}\tan^5 y_{2s}(1 + 5ip)\right] +$$
$$\alpha_2^4\left[\tfrac{247}{352800}\tan y_{2s}(1 + ip) + \tfrac{10379}{183708000}\tan^3 y_{2s}(1 + 3ip)\right] - \frac{71\alpha_2^6}{529200}\tan y_{2s}(1 + ip)$$

$$b_8^* = \tfrac{1}{40320} + \tfrac{97}{725760}\tan^2 y_{2s}(1 + 2ip) + \tfrac{1}{3840}\tan^4 y_{2s}(1 + 4ip) + \tfrac{1}{2560}\tan^6 y_{2s}(1 + 6ip) +$$
$$\tfrac{1}{5376}\tan^8 y_{2s}(1 + 8ip) + \alpha_2^2\left[-\tfrac{1}{10080} - \tfrac{42311}{1778112000}\tan^2 y_{2s}(1 + 2ip) - \tfrac{3173}{49392000}\tan^4 y_{2s}(1 + 4ip) -\right.$$
$$\left.\tfrac{583}{16934400}\tan^6 y_{2s}(1 + 6ip)\right] + \alpha_2^4\left[\tfrac{1}{6720} + \tfrac{13589}{55566000}\tan^2 y_{2s}(1 + 2ip) - \tfrac{174173}{2939328000}\tan^4 y_{2s}(1 + 4ip)\right] +$$
$$\alpha_2^6\left[-\tfrac{1}{10080} - \tfrac{61777}{444528000}\tan^2 y_{2s}(1 + 2ip)\right] + \frac{\alpha_2^8}{40320}$$

TABLE 2

SERIES COEFFICIENTS OF THE SOLUTIONS Φ_1^*, Φ_2^* FOR THE BASIC FLOW

$U = U_s + (1 - U_s) \sin\left(\frac{y - s}{a - s}\frac{\pi}{2}\right)$ ABBREVIATION: $p = \frac{f_2}{\sin y_{2s} \cos y_{2s}}$ - Concluded

$$g_0 = 1 \qquad g_1 = \tan y_{2s} \qquad g_2 = +\frac{1}{2}\tan^2 y_{2s} + \frac{\alpha_2^2}{2} \qquad g_3 = -\frac{1}{6}\tan y_{2s} + \frac{2}{9}\alpha_2^2 \tan y_{2s}$$

$$g_4 = -\frac{1}{24}\tan^2 y_{2s} + \frac{\alpha_2^2}{36}\left(-1 + \frac{7}{4}\tan^2 y_{2s}\right) + \frac{\alpha_2^4}{24}$$

$$g_5 = \frac{1}{120}\tan y_{2s} + \frac{\alpha_2^2}{50}\left(-\tan y_{2s} - \frac{1}{72}\tan^3 y_{2s}\right) + \frac{23\alpha_2^4}{1800}\tan y_{2s}$$

$$g_6 = +\frac{1}{720}\tan^2 y_{2s} + \frac{\alpha_2^2}{1800}\left(\frac{7}{3} - \frac{13}{3}\tan^2 y_{2s} + \frac{1}{2}\tan^4 y_{2s}\right) + \frac{\alpha_2^4}{5400}\left(-11 + \frac{101}{12}\tan^2 y_{2s}\right) + \frac{\alpha_2^6}{720}$$

$$g_7 = -\frac{1}{5040}\tan y_{2s} + \frac{\alpha_2^2}{3150}\left(\frac{283}{168}\tan y_{2s} - \frac{19}{21}\tan^3 y_{2s} - \frac{1}{2}\tan^5 y_{2s}\right) +$$

$$\frac{\alpha_2^4}{226800}\left(-\frac{1213}{7}\tan y_{2s} + \frac{229}{27}\tan^3 y_{2s}\right) + \frac{11}{33075}\alpha_2^6 \tan y_{2s}$$

$$g_8 = -\frac{1}{40320}\tan^2 y_{2s} + \frac{\alpha_2^2}{6720}\left[-\frac{1}{35} + \frac{961}{840}\tan^2 y_{2s} + \frac{451}{420}\tan^4 y_{2s} + \frac{13}{24}\tan^6 y_{2s}\right] +$$

$$\frac{\alpha_2^4}{25200}\left[\frac{13}{7} - \frac{883}{567}\tan^2 y_{2s} + \frac{473}{7776}\tan^4 y_{2s}\right] + \frac{\alpha_2^6}{1058400}\left[-61 + \frac{307}{12}\tan^2 y_{2s}\right] + \frac{\alpha_2^8}{40320}$$

$$h_0 = 0 \qquad h_1 = -1 - 2\tan^2 y_{2s} + \alpha_2^2 \qquad h_2 = -\frac{7}{4}\tan y_{2s} - \frac{19}{8}\tan^3 y_{2s} - \frac{1}{6}\alpha_2^2 \tan y_{2s}$$

$$h_3 = \frac{1}{4} + \frac{5}{25}\tan^2 y_{2s} - \frac{7}{24}\tan^4 y_{2s} - \frac{1}{18}\alpha_2^2\left(7 + \frac{67}{6}\tan^2 y_{2s}\right) + \frac{1}{6}\alpha_2^4$$

$$h_4 = \frac{59}{288}\tan y_{2s} + \frac{1}{3}\tan^3 y_{2s} + \frac{7}{64}\tan^5 y_{2s} + \frac{1}{1080}\alpha_2^2\left(-227\tan y_{2s} + \frac{1329}{4}\tan^3 y_{2s}\right) - \frac{1}{45}\alpha_2^4 \tan y_{2s}$$

$$h_5 = -\frac{5}{288} - \frac{23}{720}\tan^2 y_{2s} - \frac{1}{64}\tan^4 y_{2s} - \frac{1}{60}\tan^6 y_{2s} + \frac{1}{1800}\alpha_2^2\left[71 + \frac{6019}{60}\tan^2 y_{2s} - \frac{253}{60}\tan^4 y_{2s}\right] -$$

$$\frac{1}{1800}\alpha_2^4\left(53 + \frac{2291}{30}\tan^2 y_{2s}\right) + \frac{1}{120}\alpha_2^6$$

$$h_6 = -\frac{157}{25920}\tan y_{2s} - \frac{5}{1152}\tan^3 y_{2s} + \frac{59}{5760}\tan^5 y_{2s} + \frac{11}{1920}\tan^7 y_{2s} + \frac{1}{7200}\alpha_2^2\left[\frac{61721}{630}\tan y_{2s} + \frac{1093}{7}\tan^3 y_{2s} + \frac{47}{42}\tan^5 y_{2s}\right]$$

$$\frac{1}{324000}\alpha_2^4\left[\frac{17599}{7}\tan y_{2s} + \frac{321883}{81}\tan^3 y_{2s}\right] - \frac{71}{75600}\alpha_2^6 \tan y_{2s}$$

$$h_7 = \frac{11}{25920} - \frac{97}{362880}\tan^2 y_{2s} - \frac{11}{2880}\tan^4 y_{2s} - \frac{7}{1440}\tan^6 y_{2s} - \frac{29}{13440}\tan^8 y_{2s} +$$

$$\frac{1}{23520}\alpha_2^2\left[-\frac{3253}{90} - \frac{1069}{4725}\tan^2 y_{2s} + \frac{221}{14}\tan^4 y_{2s} - \frac{1}{3}\tan^6 y_{2s}\right] +$$

$$\frac{1}{25200}\alpha_2^4\left[\frac{667}{14} + \frac{4239877}{59535}\tan^2 y_{2s} - \frac{111899}{14580}\tan^4 y_{2s}\right] + \frac{1}{33075}\alpha_2^6\left[-\frac{491}{16} - \frac{4327}{105}\tan^2 y_{2s}\right] + \frac{\alpha_2^8}{5040}$$

TABLE 3

VALUES OF THE DIFFERENTIAL QUOTIENTS OF THE REAL AND OF THE IMAGINARY PART OF THE FUNCTION $F(\eta_0)$ WITH RESPECT TO η_0

η_0	$\frac{\partial F_r}{\partial \eta_0}$	$\frac{\partial F_i}{\partial \eta_0}$	η_0	$\frac{\partial F_r}{\partial \eta_0}$	$\frac{\partial F_i}{\partial \eta_0}$
-2	0.135	-0.226	-3.6	0.396	-0.066
-2.1	.121	-.230	-3.7	.399	-.030
-2.2	.117	-.235	-3.8	.395	-.010
-2.3	.118	-.239	-3.9	.379	-.055
-2.4	.121	-.242	-4.0	.360	-.100
-2.5	.128	-.245	-4.1	.330	-.155
-2.6	.135	-.246	-4.2	.297	-.205
-2.7	.145	-.246	-4.3	.250	-.270
-2.8	.157	-.243	-4.4	.180	-.338
-2.9	.172	-.237	-4.5	.080	-.341
-3.0	.191	-.226	-4.6	.020	-.282
-3.1	.219	-.210	-4.7	-.026	-.226
-3.2	.256	-.188	-4.8	-.045	-.182
-3.3	.296	-.162	-4.9	-.057	-.150
-3.4	.340	-.133	-5.0	-.062	-.118
-3.5	.380	-.102			

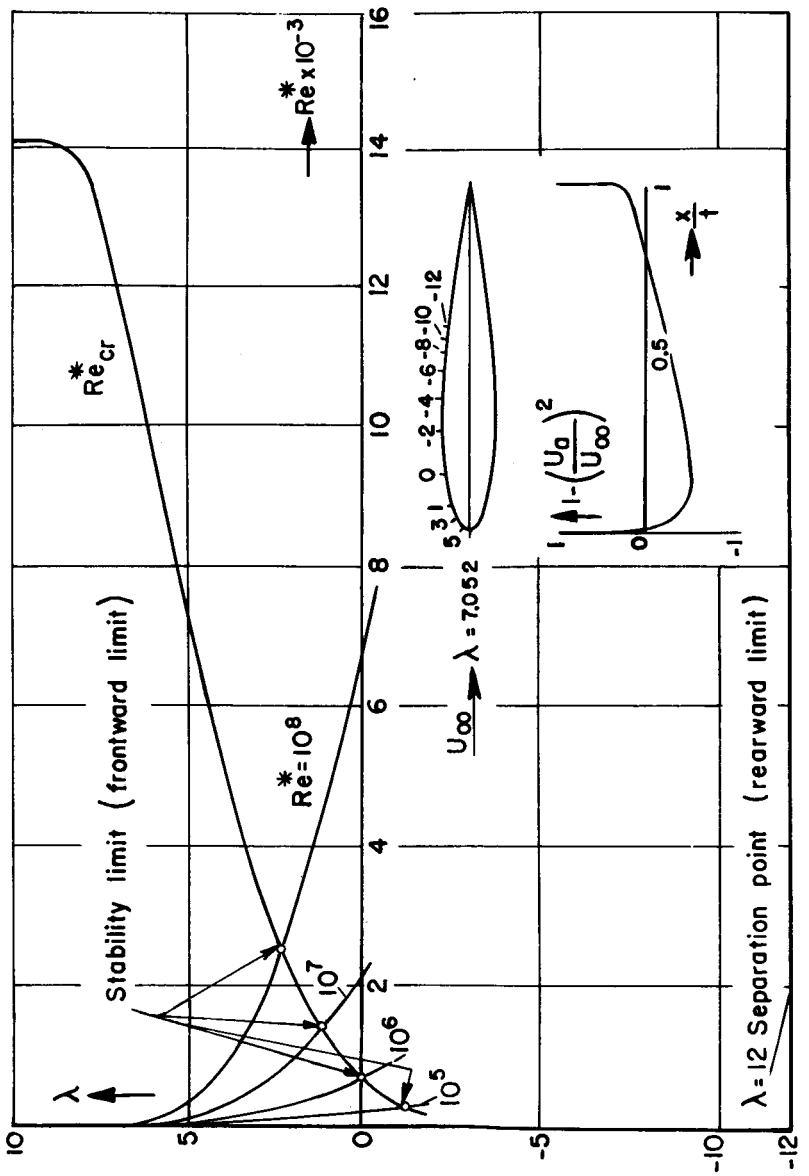

Figure 1.- Frontward limit (stability limit) and rearward limit (separation point) for the transition point on a cylindrical body.

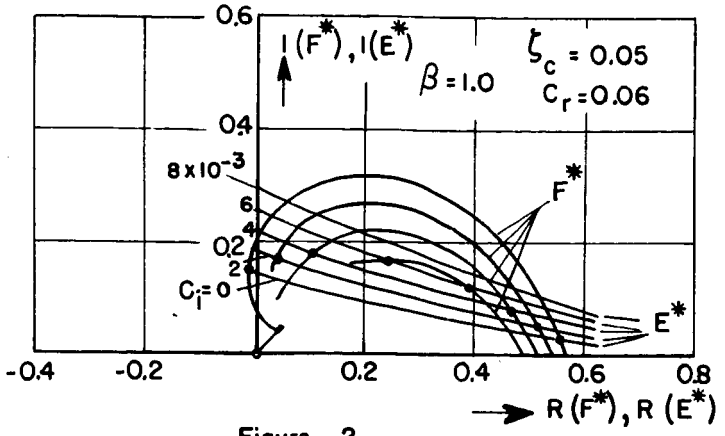

Figure 2

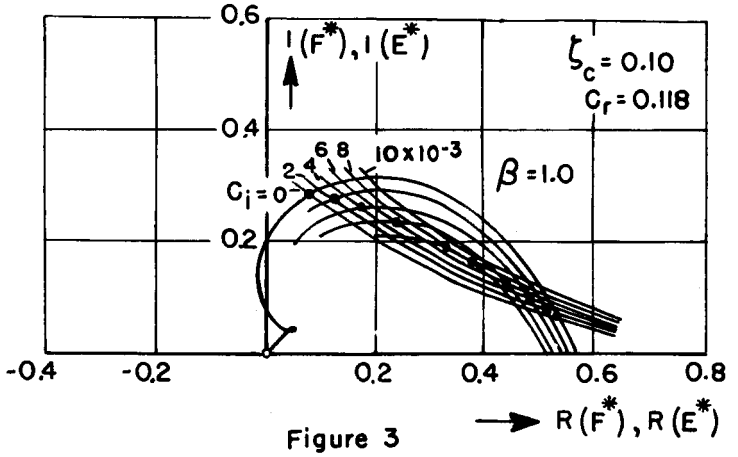

Figure 3

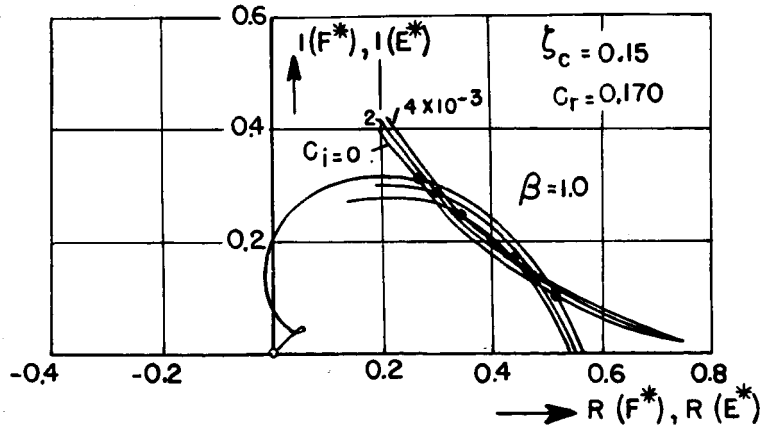

Figure 4

Figures 2, 3, and 4.- Polar diagrams for determination of the curves of constant excitation.

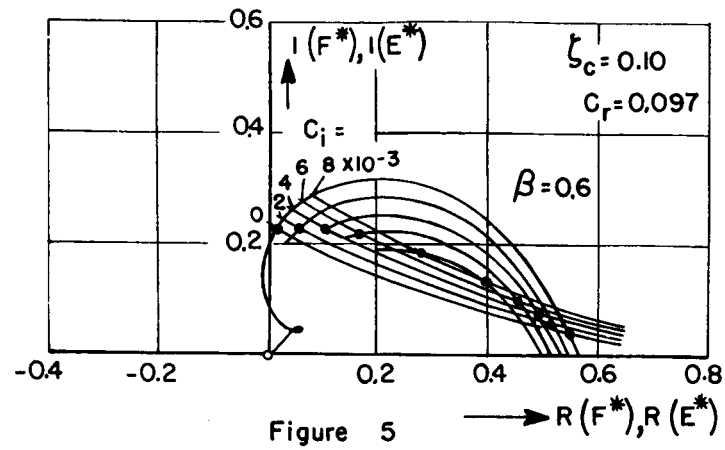

Figure 5

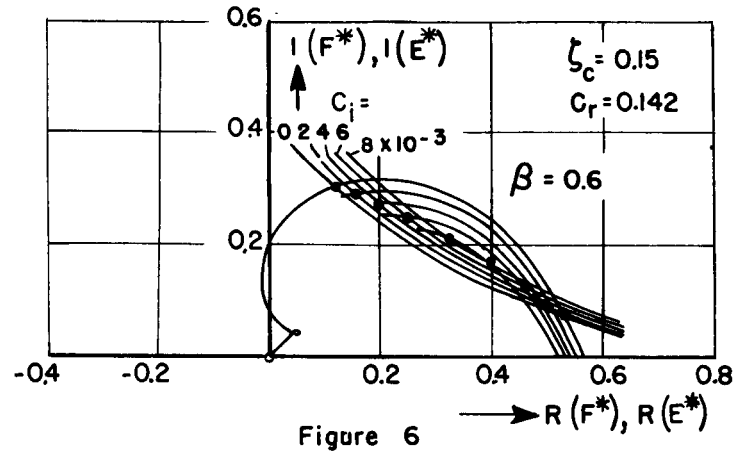

Figure 6

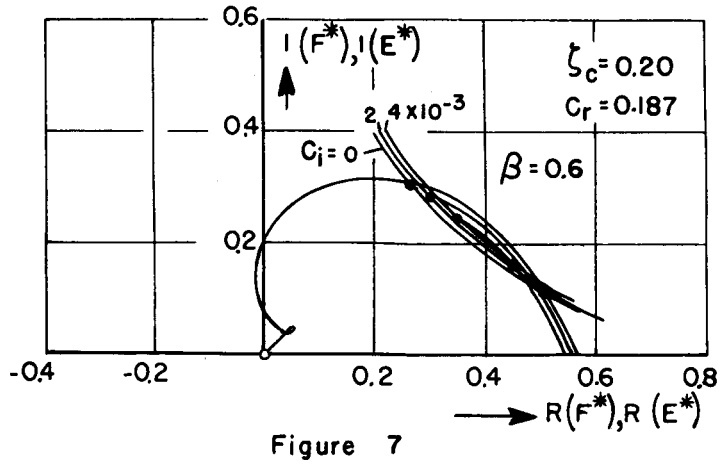

Figure 7

Figures 5, 6, and 7.- Polar diagrams for determination of the curves of constant excitation.

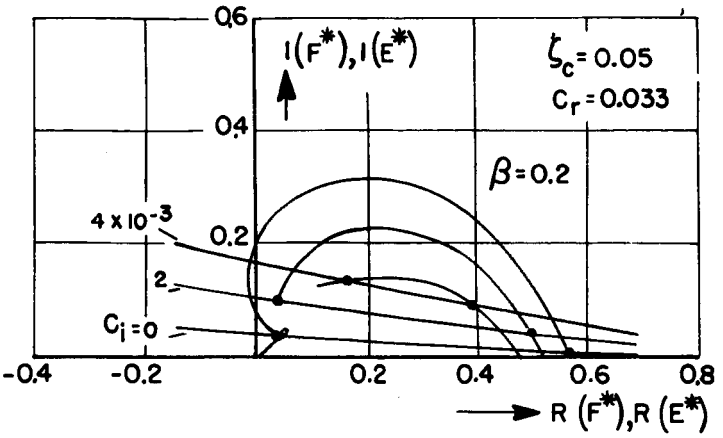

Figure 8

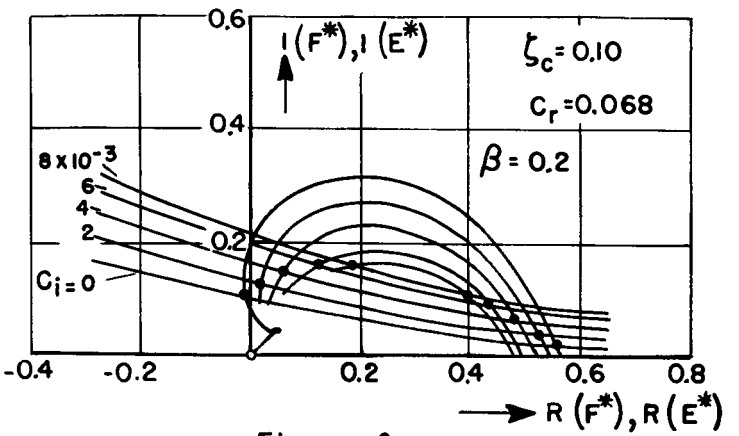

Figure 9

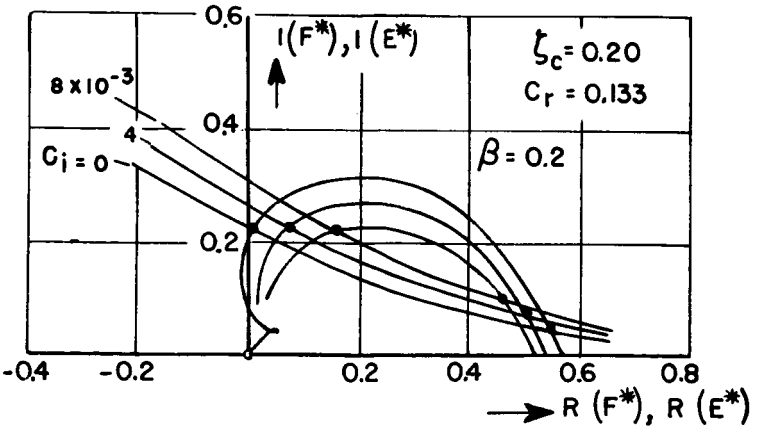

Figure 10

Figures 8, 9, and 10.- Polar diagrams for determination of the curves of constant excitation.

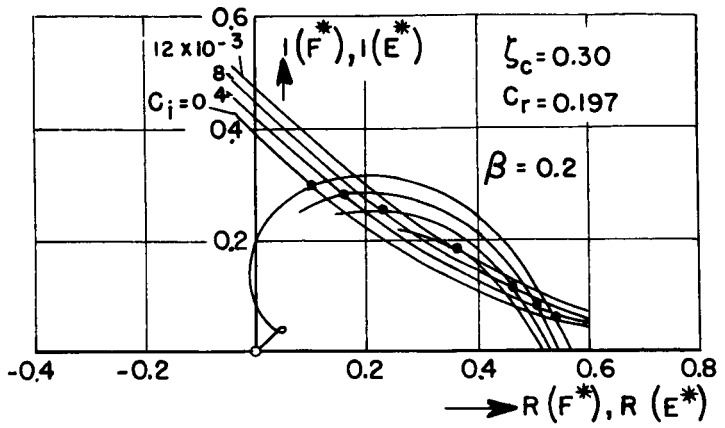

Figure 11

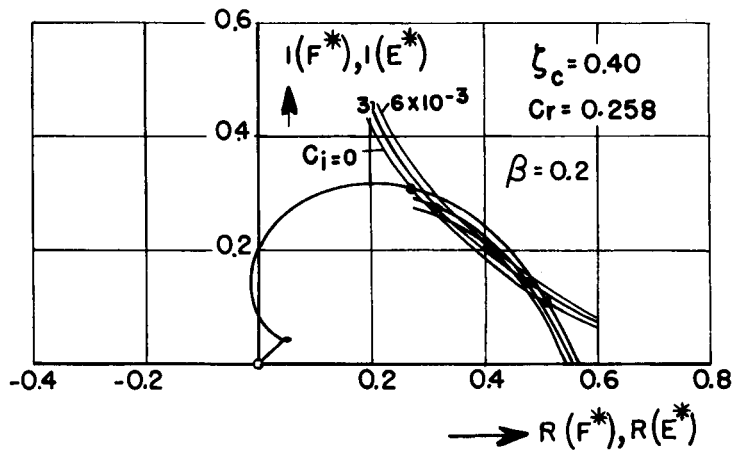

Figure 12

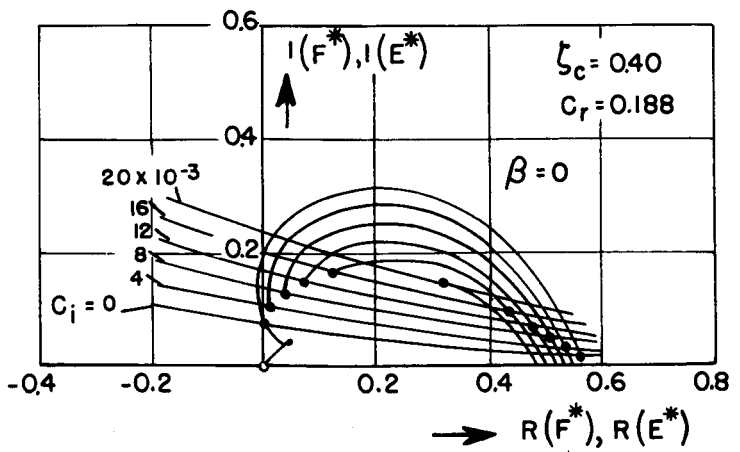

Figure 13

Figures 11, 12, and 13.- Polar diagrams for determination of the curves of constant excitation.

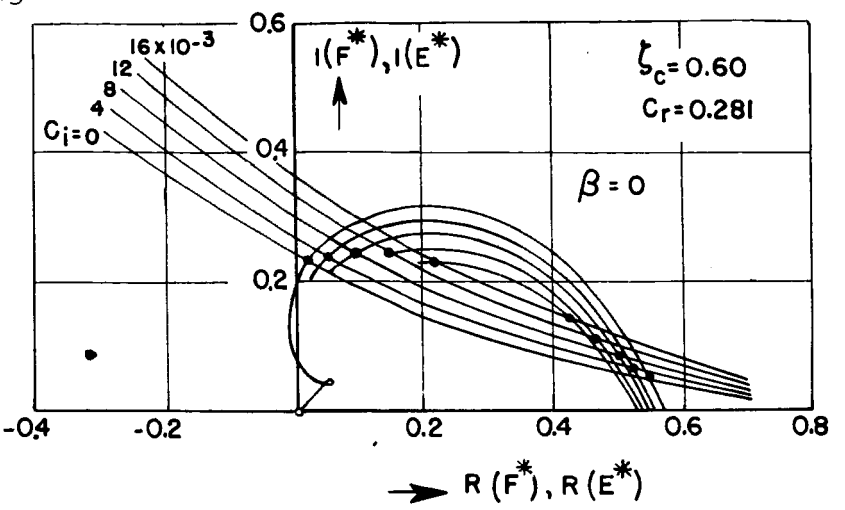

Figure 14

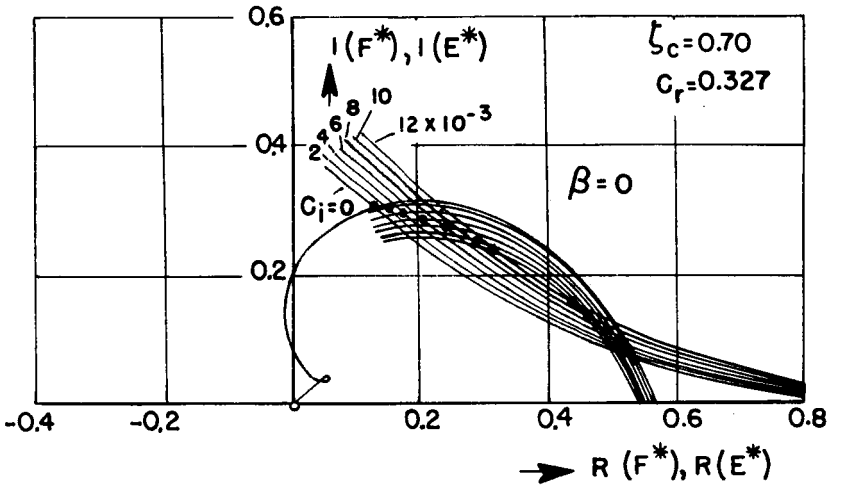

Figure 15

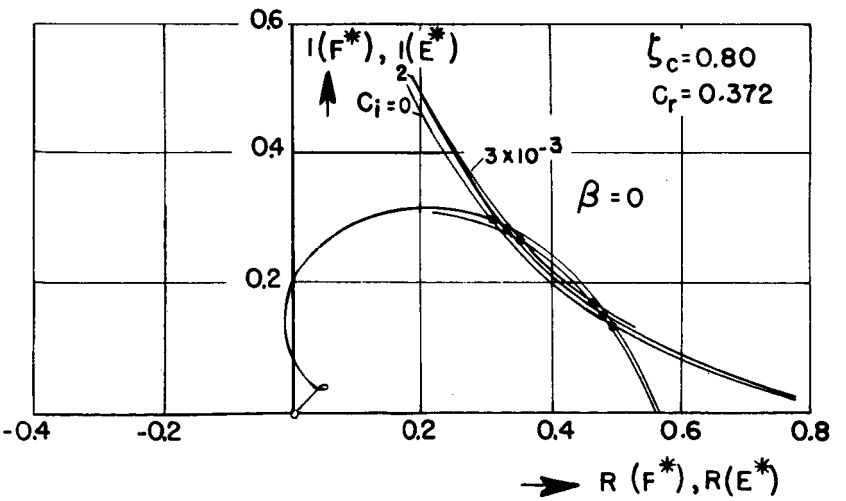

Figure 16

Figures 14, 15, and 16.- Polar diagrams for determination of the curves of constant excitation.

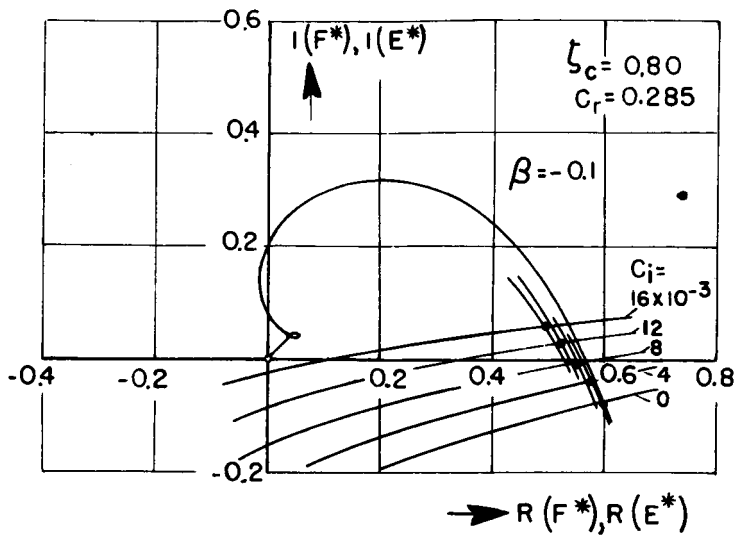

Figure 17

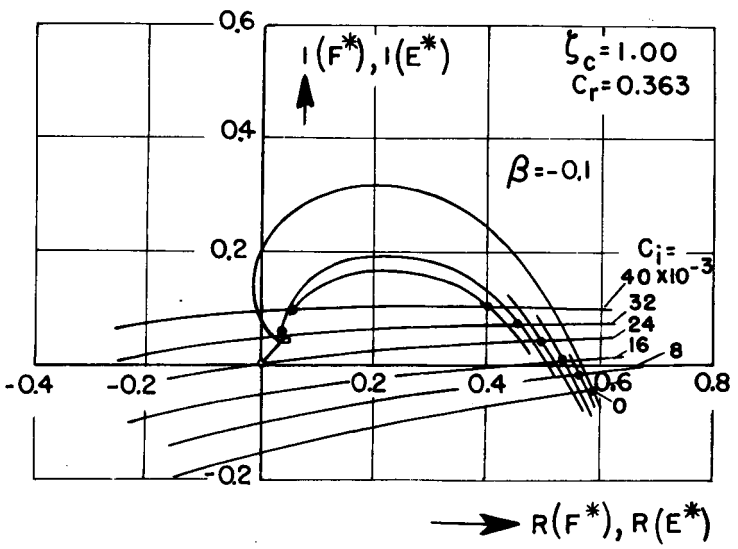

Figure 18

Figures 17 and 18.- Polar diagrams for determination of the curves of constant excitation.

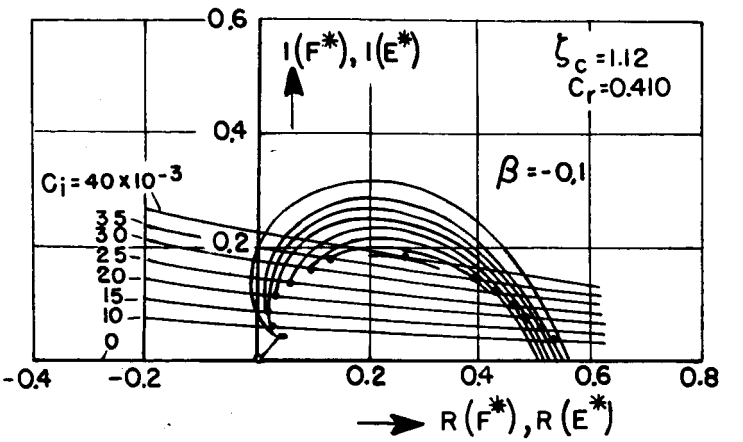

Figure 19

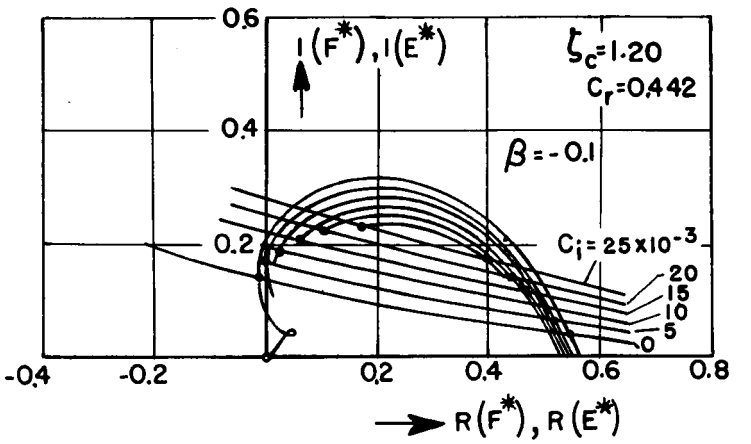

Figure 20

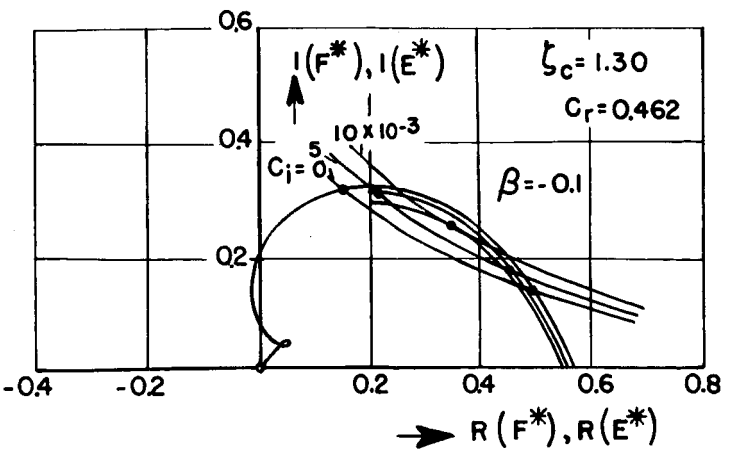

Figure 21

Figures 19, 20, and 21.- Polar diagrams for determination of the curves of constant excitation.

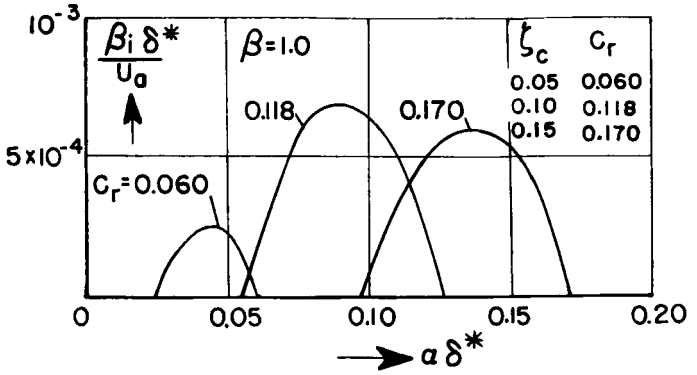

Figure 22

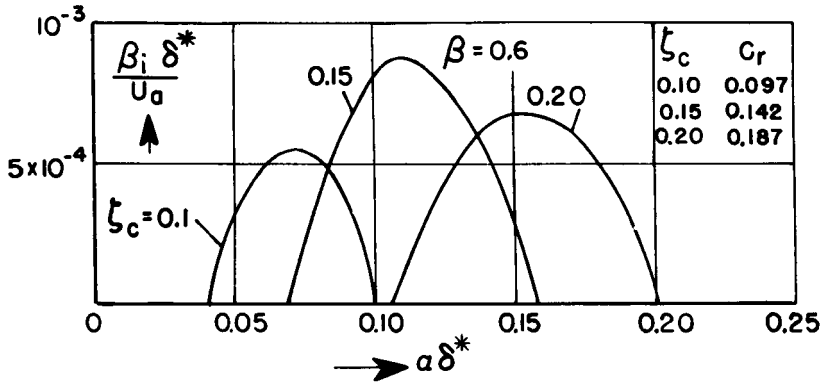

Figure 23

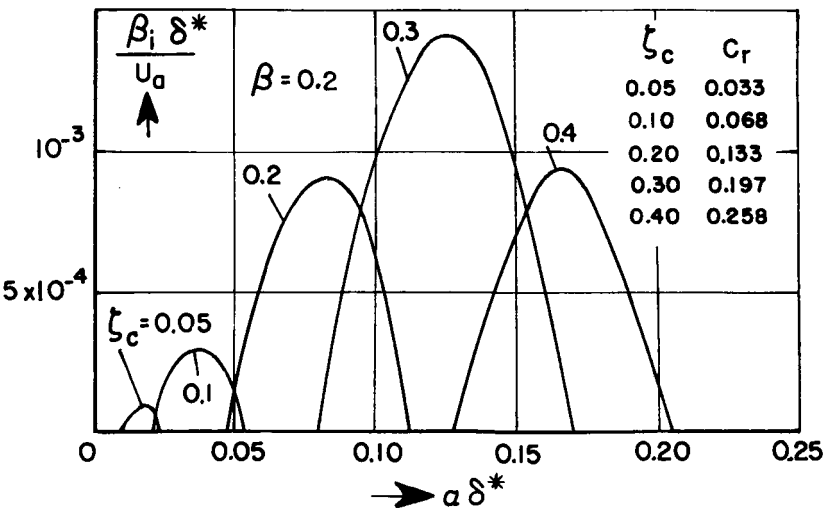

Figure 24

Figures 22, 23, and 24.- The excitation $\frac{\beta_i \delta^*}{U_a}$ as a function of the reciprocal perturbation wave length $\alpha = \frac{2\pi}{\Lambda}$ for constant critical velocity c_r.

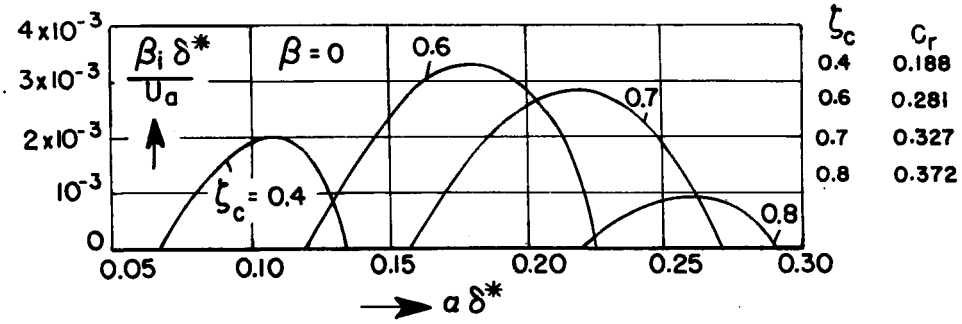

Figure 25

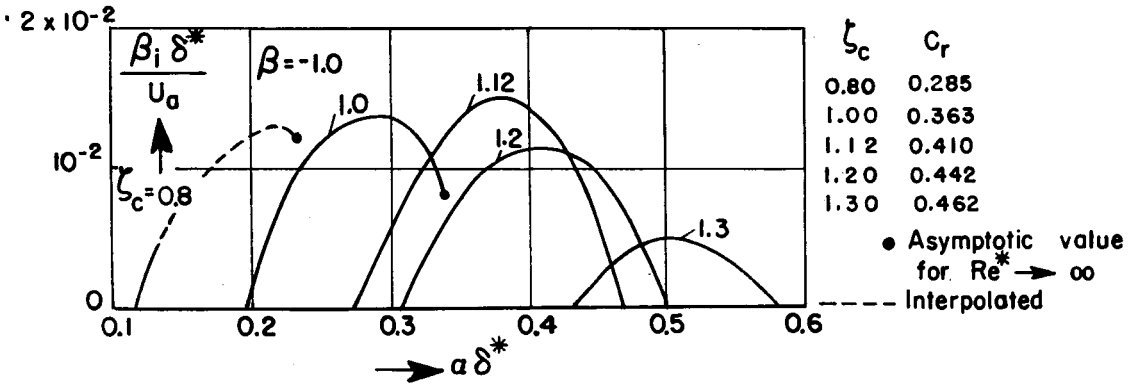

Figure 26

Figures 25 and 26.- The excitation $\frac{\beta_i \delta^*}{U_a}$ as a function of the reciprocal perturbation wave length $\alpha = \frac{2\pi}{\Lambda}$ for constant critical velocity c_r.

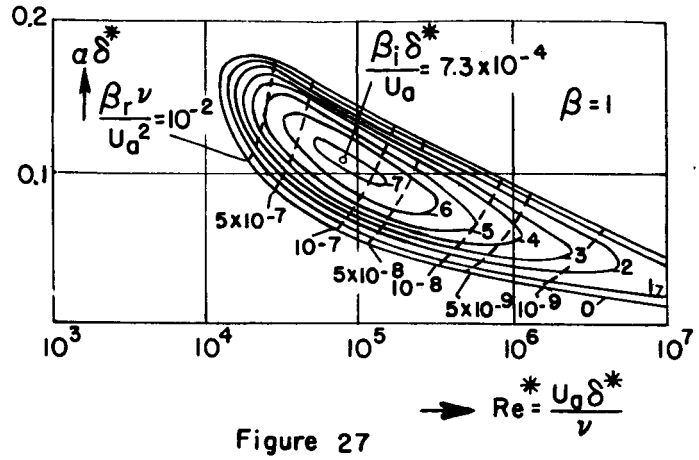

Figure 27

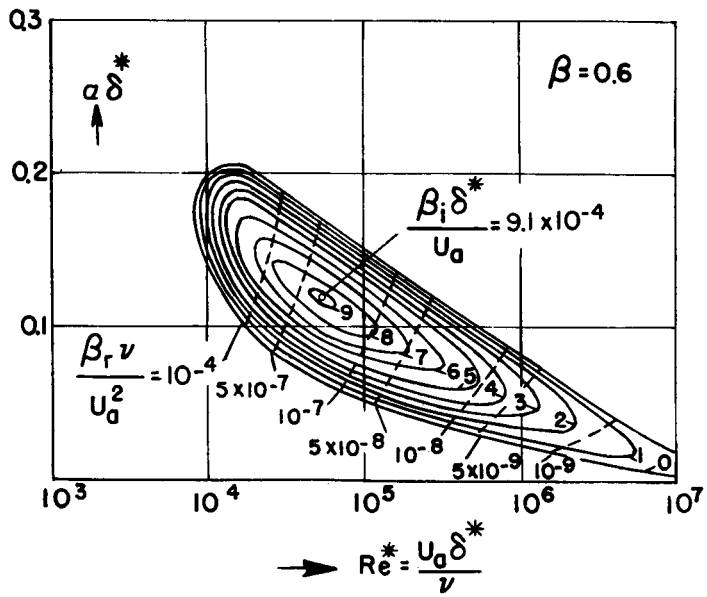

Figure 28

Figures 27 and 28.- The curves of constant excitation in the instability regions of a few laminar boundary-layer profiles.

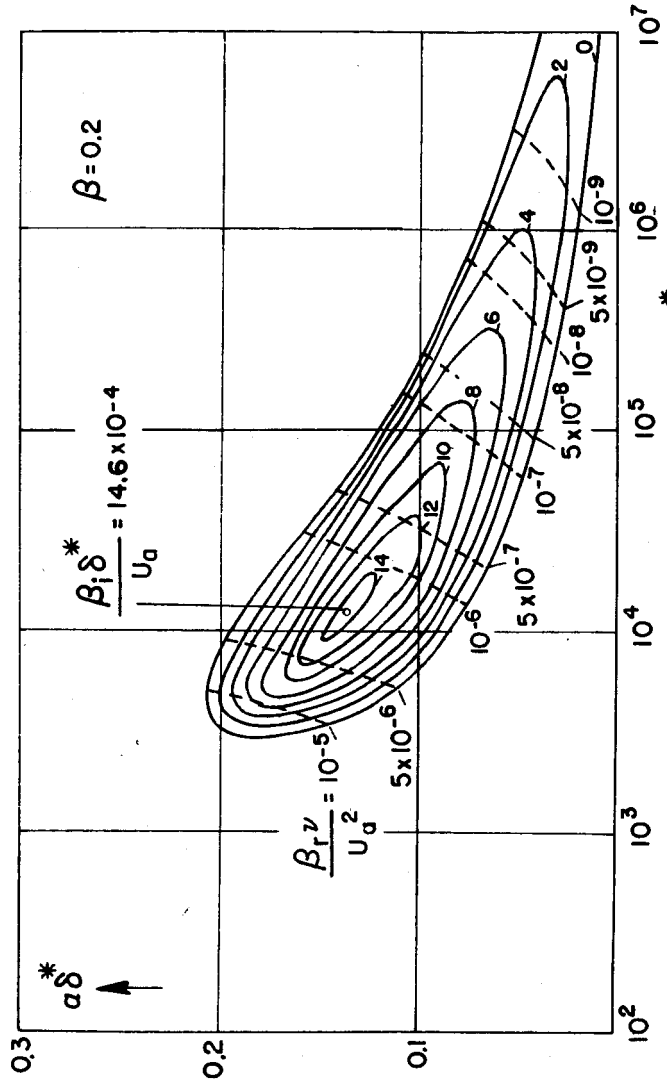

Figure 29.- The curves of constant excitation in the instability regions of a few laminar boundary-layer profiles.

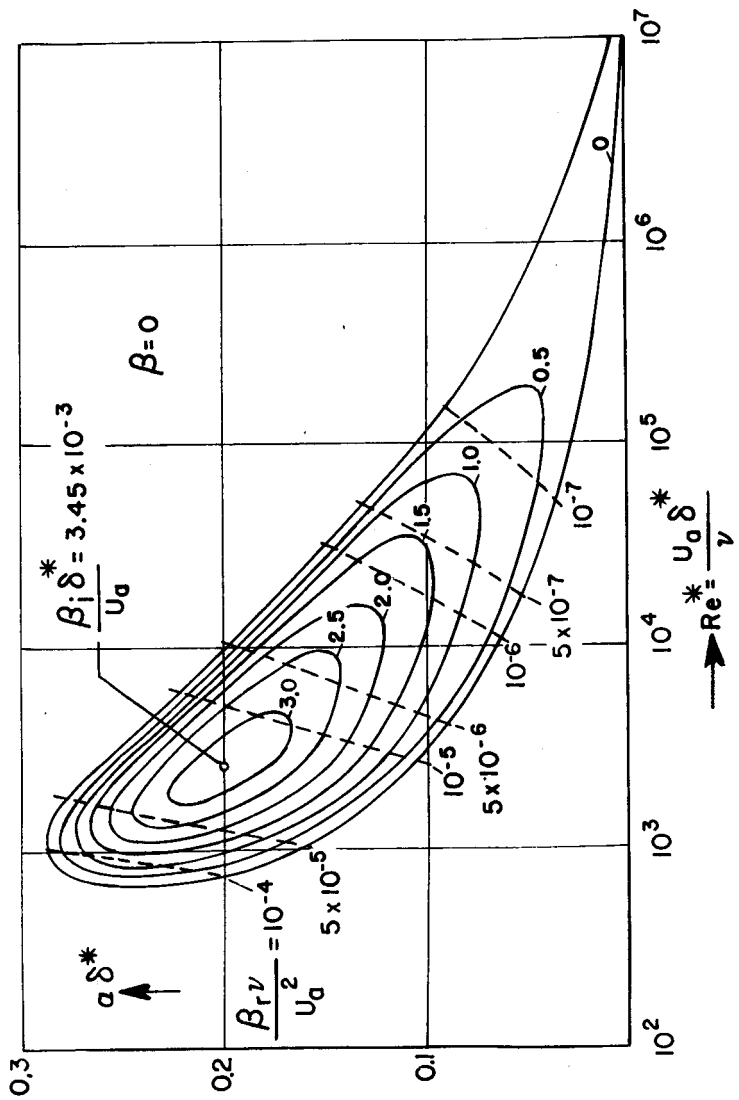

Figure 30.- The curves of constant excitation in the instability regions of a few laminar boundary-layer profiles.

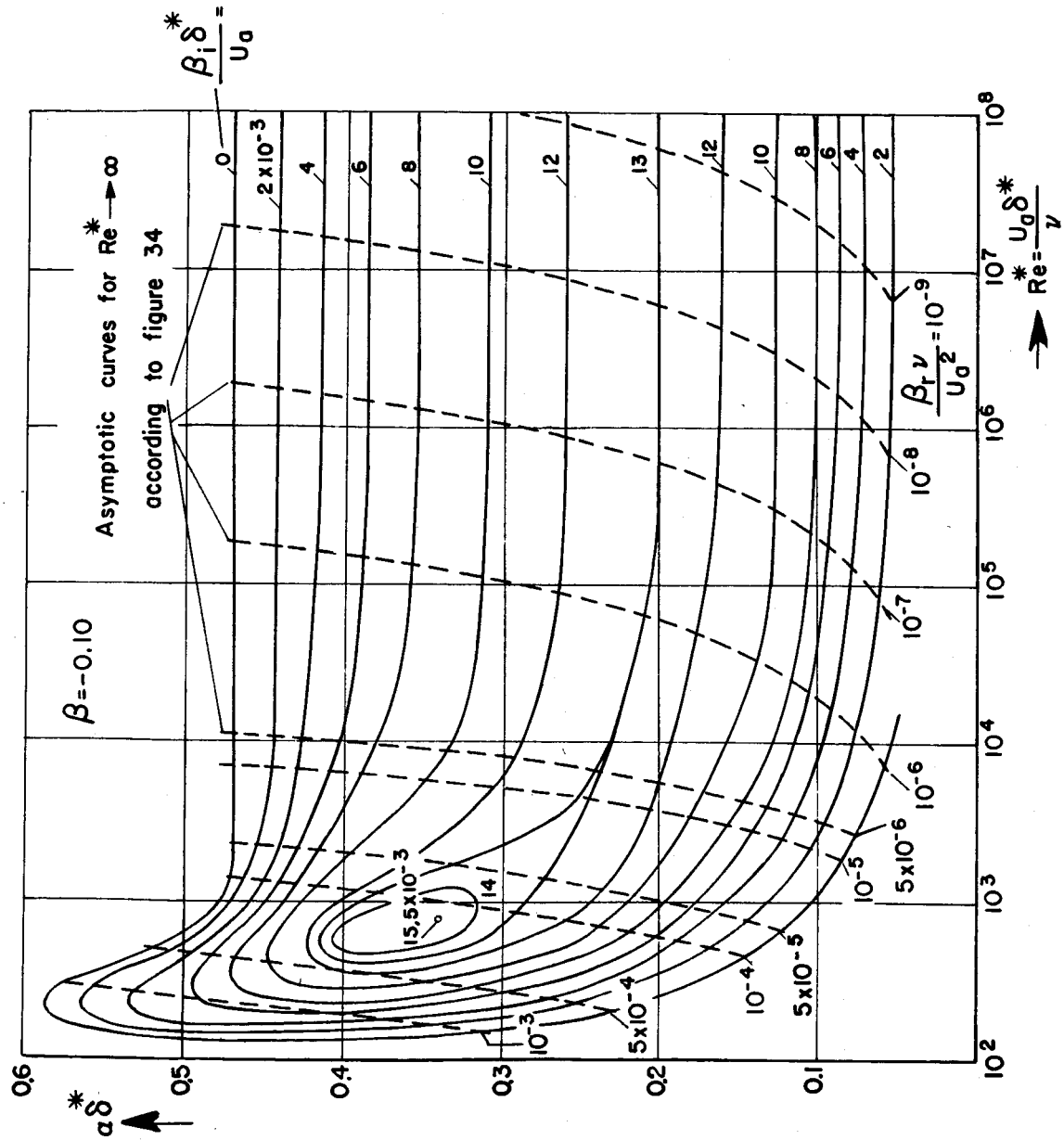

Figure 31.- The curves of constant excitation in the instability regions of a few laminar boundary-layer profiles.

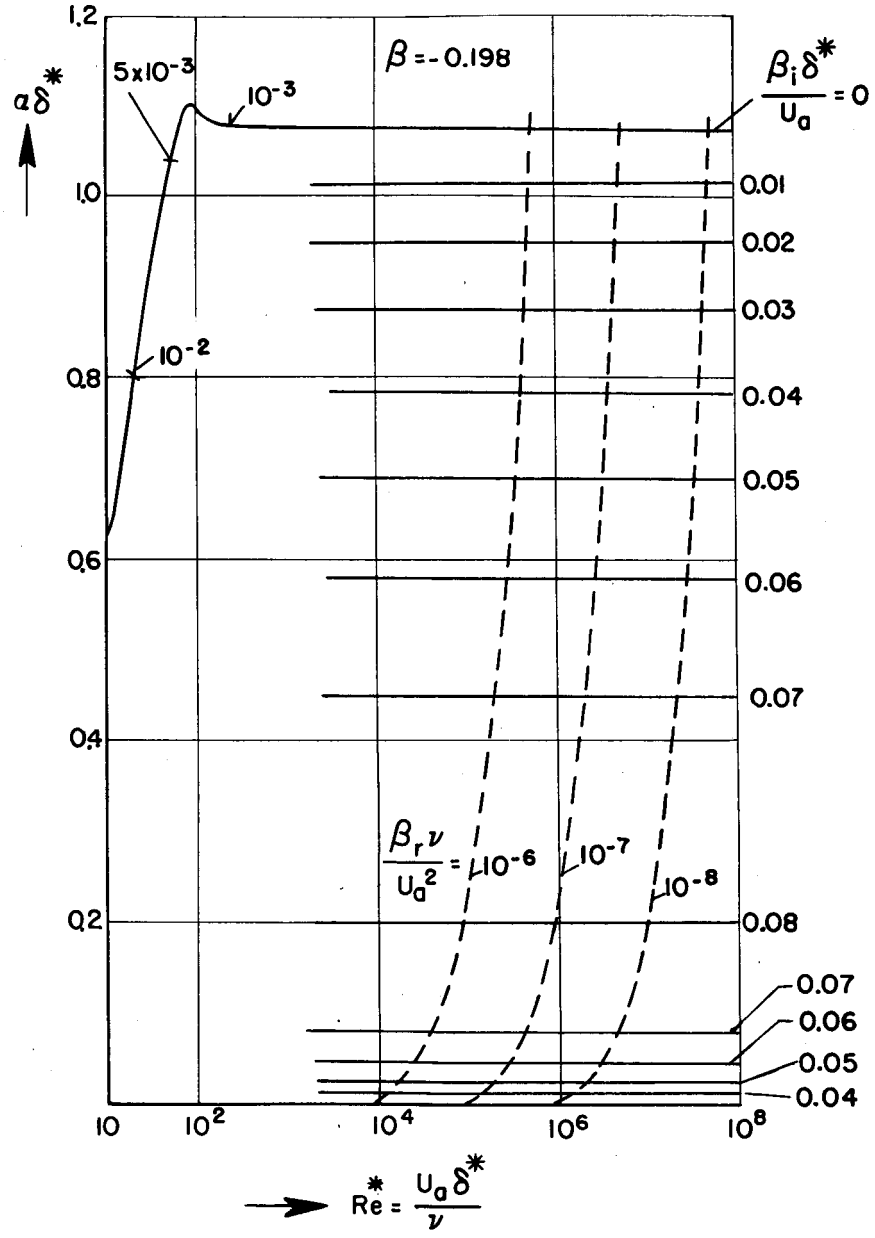

Figure 32.- The curves of constant excitation in the instability regions of a few laminar boundary-layer profiles.

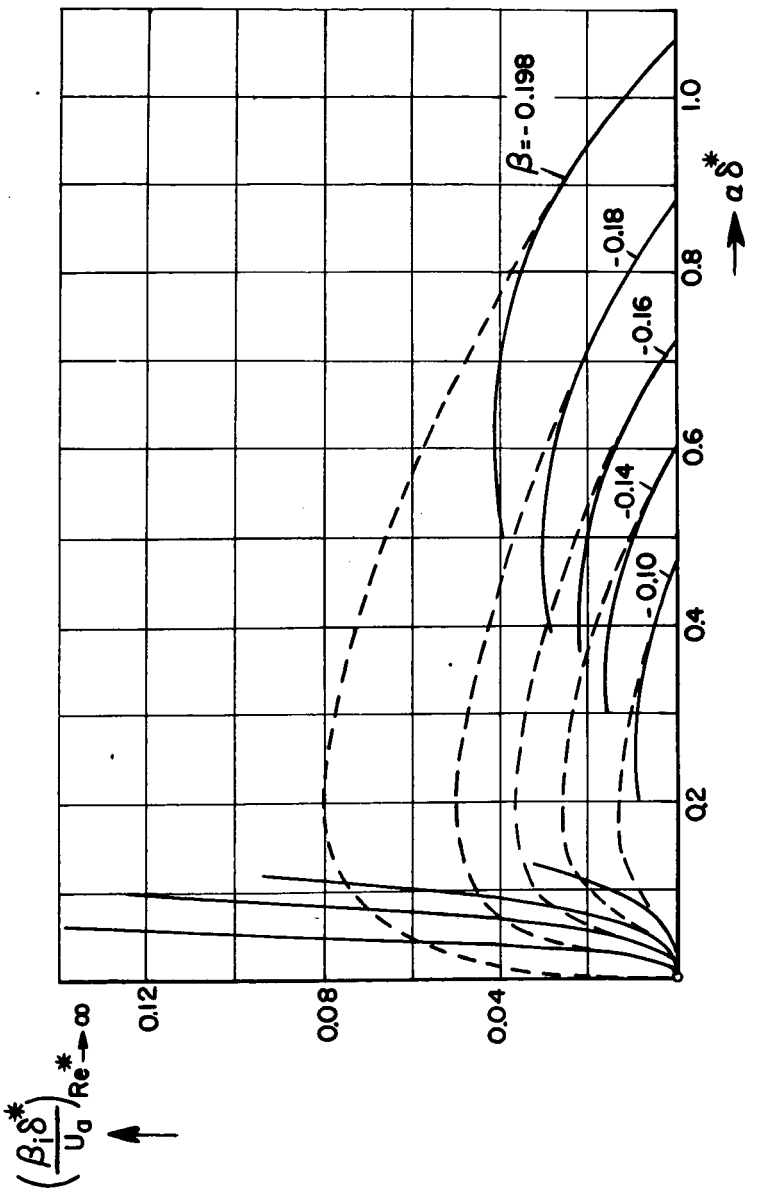

Figure 33.- The excitation $\frac{\beta_i \delta^*}{U_a}$ for boundary-layer profiles in the region of increasing pressure for $Re^* \longrightarrow \infty$.

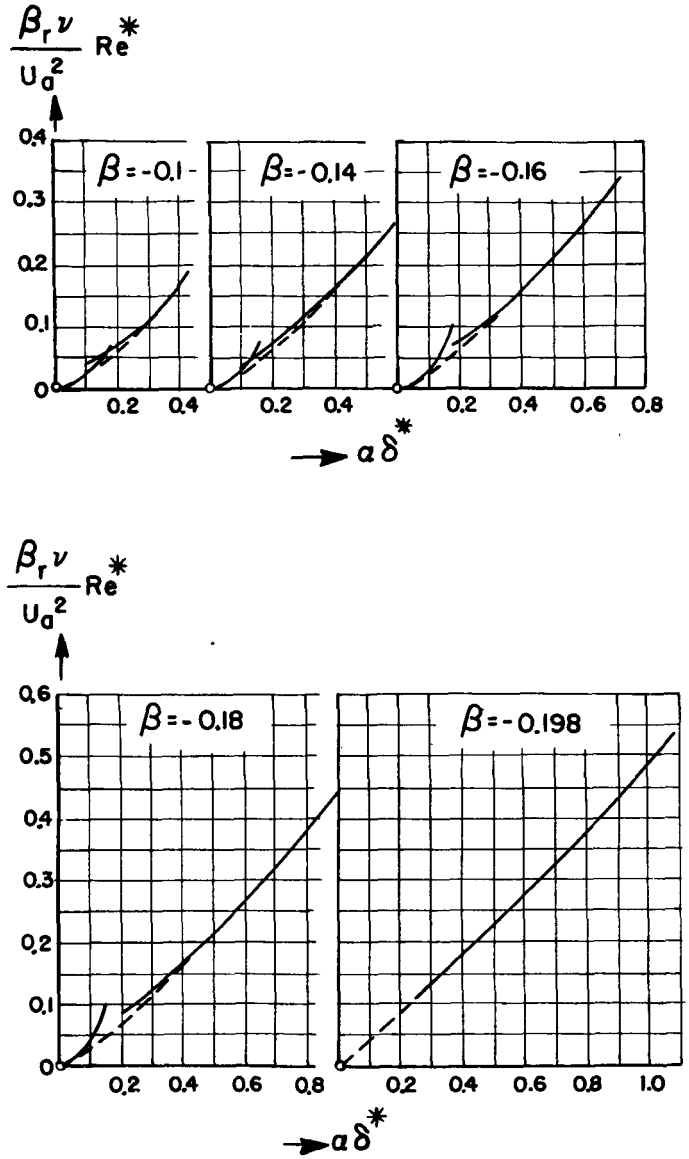

Figure 34.- The circular time frequency $\frac{\beta_r \nu}{U_a^2} Re^*$ for boundary-layer profiles in the region of increasing pressure for $Re^* \longrightarrow \infty$.

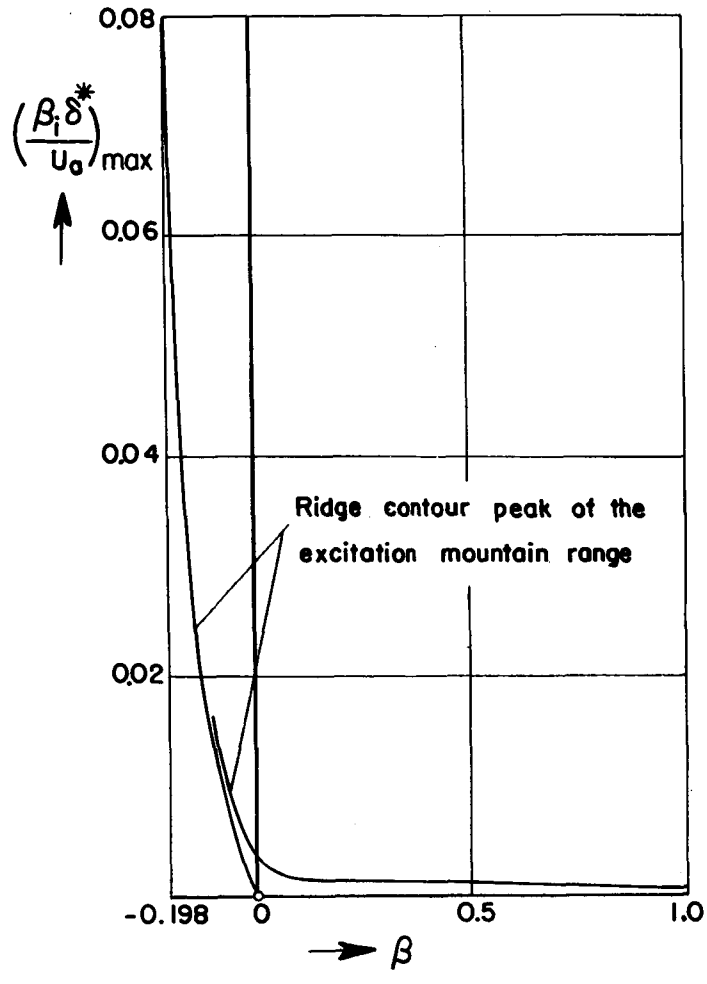

Figure 35.- The maximum excitation $\left(\frac{\beta_i \delta^*}{U_a}\right)_{max}$ as a function of the form parameter β of the laminar boundary-layer profiles.